

TECHNICAL AND ECONOMIC EVALUATION OF A NEW PROCESS FOR CO-LIQUEFYING COAL AND SCRAP TIRES

Anthony Warren and Mahmoud El-Halwagi
Chemical Engineering Department
Auburn University

Contract: DE-FC22-93PC93053
Period of Performance: May 1, 1993 - April 31, 1994

ABSTRACT- The objective of this work is to assess the technical and economic feasibility of a new process for co-liquefying coal and scrap tires. This assessment is based on incorporating recent experimental data on rubber/coal liquefaction within a conceptual process framework. A preliminary design was developed to co-liquefy 10,000 scrap tires per day with 75 tons per day of coal. The plant products include hydrocarbon gases, naphtha, jet fuel and diesel fuel. Material and energy balances along with plant-wide simulation were conducted for the process. These results were used to undertake a preliminary cost-estimation study. It was found that the annual sales of the process are slightly less than the annual production cost (including depreciation). However, the return on investment for the process is not high enough. The co-liquefaction process has also been compared to other technologies for utilizing scrap tires. It was found that co-liquefaction offers higher gross profit per tire than combustion in power plants and cement kilns. Nonetheless, co-liquefaction entails longer payback periods than the two other technologies.

1. INTRODUCTION

One of the most serious challenges facing our nation is the availability of cost-effective, stable energy sources. This problem is particularly compounded in light of the dwindling petroleum resources. In this context, the abundant coal reserves in the United States can provide a sustainable energy source. To date, commercial-scale coal liquefaction is not economically feasible in the United States. The current low

prices of oil present a major hurdle for the economic feasibility of coal liquefaction. Indeed, it seems that for coal liquefaction to be commercially feasible, a fundamental change in the technology should be affected. Such a technological change may be realized by incorporating cheaper sources of energy in the coal liquefaction process. An abundant source of low-cost energy is scrap tires. Each year, 244 million scrap tires are generated in the United States. In addition, about 2 billion scrap tires have accumulated in landfills, stockpiles or illegal dumps (U.S. EPA, 1991). They pose various environmental, health and safety problems. These problems have motivated many states to regulate the disposal of scrap tires and to charge tipping fees for collecting scrap tires. These charges vary depending on whether tires are landfilled whole or shredded. At present, several technologies are available for utilizing scrap tires. These technologies include the conversion of scrap tires into usable forms of energy and the processing of tires in specialty applications. For instance, scrap tires can be used as a source of fuel for combustion in power plants and cement kilns. Crumb rubber may be employed in several applications such as producing asphalt for highways. Some of the newer technologies include the use of scrap tires in manufacturing high-performance rubberized flooring. These technologies help address part of the environmental problems connected with the disposal of the scrap tires. Nonetheless, no technology has been able to rise to the point of tackling a significant portion of the scrap tires generated annually. Furthermore, none of these technologies is capable of producing liquid transportation fuels in a cost-effective manner. The use of transportation fuels in the United States is a fundamental aspect in our way of life. Alternative means of feasibly producing transportation fuels must be found.

Recent research efforts (Farcasiu, 1993; Farcasiu and Smith, 1992 and 1991) have shown that it is possible on a lab scale to co-liquefy coal and scrap tires into liquid fuel. This process is achieved by subjecting coal and tire to relatively high temperature and pressure (e.g. 825 °F and 2200 psi) in the presence of hydrogen. Experiments are reported to yield hydrocarbon mixtures. Similar to traditional coal liquefaction experiments, three fractions of liquid/solid products were reported. These fractions can be classified into oils, asphaltenes and preasphaltenes. The preasphaltenes are found to be insoluble in methylene chloride. This fraction contains unreacted coal, repolymerized coal-like masses and virtually all of the carbon black and inorganic matter from tires. The methylene chloride soluble, heptane insoluble fraction contains the asphaltenes which are the heavy liquids yielded from liquefaction. The oil fraction is the most important product with respect to potential use as transportation fuels. Oils are designated as the fraction of product which is methylene chloride and heptane soluble. This fraction can then be refined to yield naphtha, light, middle, and heavy distillates.

The objective of this paper is to provide a technical and economic assessment of the process of co-liquefying coal and scrap tires. First, the current technologies for utilizing scrap tires will be reviewed. Then, the problem to be addressed in this work will be formally stated. A process flowsheet will be conceptualized. Next, the material and energy balances for the process along with a plant-wide simulation using the software ASPEN PLUS will be undertaken. Finally, the economic aspects of the process will be analyzed.

2. SCRAP TIRE DISPOSAL AND CONVERSION

At present, there are serious environmental problems attributed to the annual generation of 244 million scrap tires in the United States. Furthermore, Approximately two billion scrap tires are currently scattered throughout the nation in landfills, stockpiles or illegal dumps (EPA, 1991). These tires pose various problems. They provide breeding grounds for mosquitoes. In addition, piles of scrap tires constitute major fire hazards. They also take up valuable land filling space, especially around cities. The foregoing problems have led to several legislations affecting the disposal of scrap tires. Currently, many states have laws mandating the shredding of tires prior to land filling. The costs associated with landfilling scrap tires (whole or shredded) vary throughout the country. These costs range from \$0.35/tire in the West Coast to \$1.08/tire in the North East of the United States. Many states have now imposed surcharges on the retail prices of new tires to account for future disposal costs. For instance, Florida, Kentucky, Maine, Nebraska, Oklahoma and Oregon require a surcharge of one dollar of its retail cost per tire for disposal. In Arizona, a two percent sales tax is imposed on the retail of tires to be allocated for disposal.

It is worth discussing current disposal and conversion methods employed in tackling scrap tires. As has been mentioned earlier, 244 million scrap tires are generated each year in the United States. Almost 78% of these scrap tires are landfilled, stockpiled or illegally dumped. The current leading technique for utilizing scrap tires is combustion. About 11% of the scrap tires in the United States are burnt primarily in power plants, cement kilns and pulp and paper mills. This method is motivated by the relatively high heat of combustion (~300,00 Btu/tire). At present, two processes employ tire combustion in power plants. The first power plant in the

United States to use scrap tires operates in Modesto, California (Valenti, 1991). It burns about five million tires/year and generates 14 MW of power. The second power plant is located in Sterling, Connecticut which burns 11 million tires/year and generates 33 MW of power. Scrap tires can also be burned in cement kilns. At present, seven cement kilns in the United States use 14 million tires/year. This number may potentially grow to 40 kilns burning up to 80 million scrap tires/year. The process of burning scrap tires as a source of fuel in kilns is relatively straightforward. Therefore, it involves low fixed and operating costs. In addition, the iron which exists in the scrap tires is used in cement manufacture. The high operating temperature (2600 °F), the long residence time and the excess oxygen environment minimize the generation of hazardous species such as dioxins and furans.

Another alternative for utilizing scrap tires is the use of crumb rubber as an additive for asphalt. This option is particularly important in light of the "Intermodal Surface Transportation Efficiency Act" which has been recently passed by the United States Congress. According to this Act, asphalt pavements should contain a minimum percentage of recycled rubber. This percentage is five percent for 1994, 10% for 1995, 15% for 1996 and 20% for 1997. This alternative may use up to 80 million tires/year. States that do not comply with this act may lose part of their federal funding for highways. Asphalt-rubber costs almost twice as much as standard asphalt. In addition, recycle of asphalt-rubber may not be feasible by heating since rubber may catch fire. On the other hand, asphalt-rubber offers longer lifetime than standard asphalt, thereby providing lower cost on a life-cycle basis. Nonetheless, in many states the decision of constructing a new highway is typically based on initial cost rather than life-cycle cost.

An additional option is to liquefy rubber under high temperature and pressure into liquid fuels. A commercial-development run by Texaco started operation in December 1992 in Montebello, California (Perry, 1993). First, the shredded tires are cooked at 700 °F for 30 minutes for melting purposes and then passed through to a liquefaction reactor. A liquid hydrocarbon mixture is created as the heat breaks the vulcanization bonds formed in the tire manufacturing process. This liquid goes to a reactor for gasification into a syngas. The syngas has relatively low sulfur content due to the low sulfur content of the tires. The gasifier is operated at 2500°F and 500 - 900 psi. The syngas is used to produce electricity and is less harmful to the environment than a conventional coal-fired power plant. A gas steam is withdrawn and partially condensed to yield gas and a light oil product which can be further processed to yield gasoline, diesel oil and other feed stocks. This plant liquefies 500,000 tires/year.

3. PROBLEM STATEMENT

The problem to be addressed in this paper can be stated as follows:

Given a steady flow of 10,000 scrap tires per day, it is desired to develop a technical and economic evaluation of a process that co-liquefies the scrap tires with an equal mass of coal. The liquefaction chemistry is based upon recent reaction experiments which have demonstrated the lab-scale feasibility of the process (Farcasiu and Smith, 1993 and 1991). The technical assessment is to involve material and energy balances along with plant-wide simulation. These technical results are to be used in undertaking an economic feasibility study for the proposed process.

4. PROCESS CONCEPTUALIZATION AND SIMULATION

The first step in designing the process is to develop a conceptual flow sheet. The conceptualized process flow diagram intended to co-liquefy coal with scrap tires appears in Figure 1. The scrap tires are sent to a shredder which chips the tires and rids them of the steel belted reinforcements. Coal is first crushed then distributed to the slurry mixer and to hydrogen generation. The shredded tires and crushed coal are mixed with a recycled solvent to form a slurry. This slurry mixture is fed to a preheater. The preheated slurry is then forwarded to an adiabatically operated reactor which yields vapor, liquid and solid products. The vapor, leaving the reactor at 800 °F and 2200 psi, is first relinquished of hydrogen which is recycled back to the reactor after being mixed with the fresh hydrogen feed. The remainder of the stream is then separated into vapor and liquid products by using a flash column. The gas leaving this flash column is sent to an acid gas removal system. The remaining gas consists of light petroleum fuel gases. The hydrogen sulfide removed is processed in a Claus unit to yield elemental sulfur. The slurry leaving the reactor is first flashed in the gas oil column. The column yields a vapor product which contains most of the valuable hydrocarbon fractions. The bottom product leaving the column includes heavy hydrocarbons along with the unreacted coal, ash and tire inorganics. The vapor stream leaving the gas-oil flash column is hydrotreated and distilled to yield light, middle and heavy distillates. A hydroclone is employed to process the bottoms from the gas oil flash column. The product leaving the top of the hydroclone contains the heavy boiling point fraction (>650 °F). This fraction is recycled to the slurry mixer as a hydrogen solvent donor. Additional liquid from this fraction is removed using the Wilsonville evolved Residuum Oil Supercritical Extraction-Solid Rejection [ROSE-

Having developed a conceptual flow sheet for the process, one is now in a position to simulate the plant and conduct the necessary calculations for material and energy balances as well as other technical aspects. An average tire was assumed to weigh 16 pounds out of which one pound is steel..

Material and energy balances for the plant have been conducted. In addition, a plantwide simulation has also been undertaken using the software ASPEN Plus. Optimization of some units/systems has been carried out to minimize capital and operating costs. In order to yield an environmentally benign plant, the removal and recovery of the sulfur by-product has been achieved via a desulfurization system. Heat integration has also been done by using the pinch techniques (Linnhoff and Hindmarsh, 1982) to synthesize a heat exchange network. The detailed results of these endeavors can be found elsewhere (Warren, 1993). Figure 2 summarizes the overall material balance for the plant.

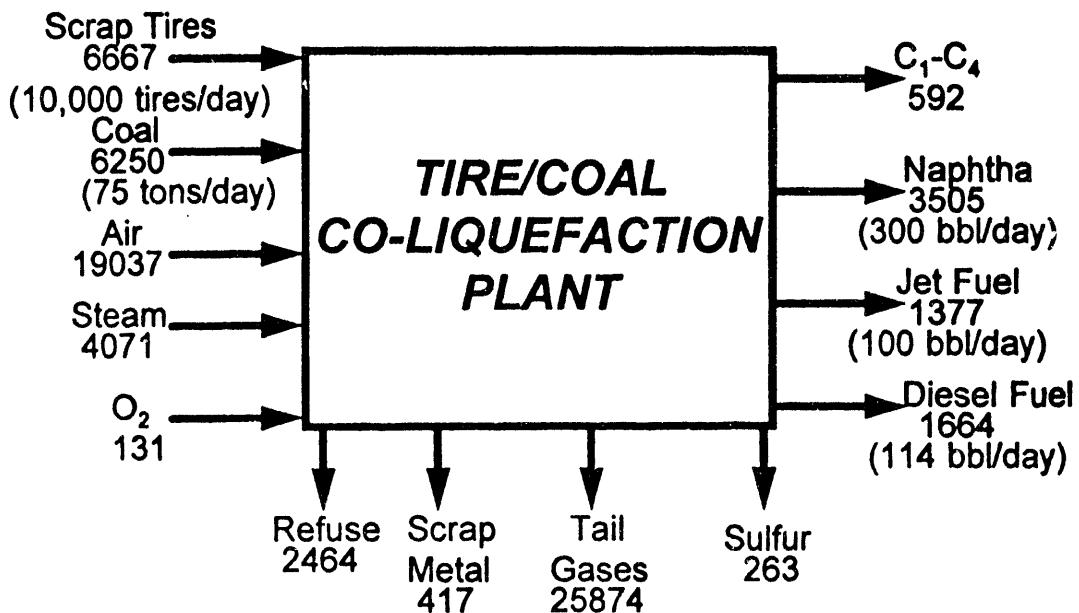


Figure 2. An Overall Material Balance for the Plant
(All Numbers are in lb/hr Unless Stated Otherwise)

5. ECONOMIC ANALYSIS

This section focuses on the economic aspects of this co-processing plant. In order to test any of the profitability criteria of the plant, one must first evaluate fixed capital investment, total capital investment, total production cost and annual revenue. These aspects along with a profitability analysis will be discussed in the following sections.

5.1. Fixed Cost Estimation

The first step in estimating the fixed cost of the plant is to evaluate the purchased equipment cost. This cost estimation is determined by relating equipment capacities to cost via data available in literature (e.g. Peters and Timmerhaus, 1991). In particular, the cost of several pieces of equipment was determined by scaling-down based on a recent Bechtel/Amoco study (US DOE-PETC, 1993). This DOE-sponsored study provides an extensive economic evaluation of direct coal-liquefaction in which Illinois #6 coal is liquefied to yield naphtha, light, middle, and heavy distillates. Design aspects throughout the plant were taken from several pre-existing liquefaction projects (Breckinridge, Wilsonville, HRI, etc.). Based on the capacity of the pieces of equipment needed in this co-liquefaction study, the cost may be calculated using the suggested Bechtel/Amoco scaling exponent of 0.71. Hence, the purchased equipment cost for the co-liquefaction plant can be evaluated. The purchased costs of the major pieces of equipment are tabulated in Table 1. As can be seen by this table, the total purchased equipment cost is \$28,683,000. The liquefaction system (reactor, ebullating pumps, etc.) is the dominant contributor to equipment cost since it accounts for \$19,680,000 (69% of the total equipment cost). This high cost is due to the very specialized design of the ebullated-bed liquefaction

Table 1. Purchased Equipment Cost of the Major Units

Equipment	Capacity, lb/hr	Cost ^a , 1000\$
Tire shredding	6250	169
Coal preparation	6250	23
Liquefaction	43750	19680
Preheater	43750	15
Gas oil flash	42136	320
H ₂ Separation	3114	70
Naphtha flash	1989	23
Hydroclone/ROSE	37507	1423
Naphtha Hydrotreater	1769	173
Gas oil Hydrotrater	4630	342
Sulfur recovery	276	4157
Distillation	4759	40
H ₂ generation	549	2248
TOTAL		28683

a-All Cost are on 2nd quarter 1993 basis.

system. From this total purchased equipment cost, the fixed capital investment and total capital investment are estimated using typical percentages for solid-liquid processing chemical plants (Peters and Timmerhaus, 1991). The resulting fixed and total capital investments are \$118 million and \$140 million, respectively. An itemized account of the elements contributing to these investment costs appears in Table 2.

Table 2. Itemized Investment Costs

Equipment	Cost, 1000 \$
Purchased equipment cost	28683
Installation (equipment)	11187
Instrumentation and controls	3729
Piping (installed)	8892
Electricity	2868
Buildings	8318
Yard improvements	2868
Service facilities	15776
Land	1721
Engineering and Supervision	9179
Construction	9752
Contractor's fee	5163
Contingency	10325
Fixed Capital Investment	118461
Working Capital Investment	21226
Total Capital Investment	139687

5.2. Shredding Cost

An important cost item is that of shredding the scrap tires. There are three major technologies used in tire shredding; mechanical, cryogenic and water-jet shredding. First, mechanical shredding has been used for some time to down size rubber tires prior to disposal. Most mechanical shredders convey the whole tires on a belt through a series of cutters or rotating shredders in order to reduce the size the tires. The most serious problem associated with mechanical shredding is that heavy erosion occurs due to the abrasion of the steel reinforcements. Also, since steel-free rubber is typically desired for further processing, separation of steel and fabrics

contained in tires is needed. This is very difficult to accomplish with the mechanically shredded chunks of tire. At present, mechanical shredding costs approximately \$0.25/tire (U. S. EPA, 1991).

Cryogenic shredding is another option for shredding. According to Moore and Aten (U. S. patent 4,813,614, 1987), the tires are first cooled to a very low temperature to render the rubber brittle. The tires are then passed through at least one crusher. It is proposed to use liquid nitrogen to cool the scrap tires to -250°F then pass them through a ball mill used for further size reduction of the brittle cold tire shreds. While the refrigerated rubber becomes brittle, the strength of steel is unaffected. Upon crushing, separation of the steel from the main stream flow is achieved by magnetic means. For the predefined flowrate of 10,000 tires/day, approximately 40 hp are needed to run the ball mill (Snow et. al, 1984). Based on heat balance, $17.325 \text{ E}+6$ Btu/day should be removed via refrigeration system. The operating cost is attributed to power requirement in the conveyor and crusher and the cost of liquid nitrogen to refrigerate the tires. Thus, operating cost is calculated to be \$333, 245/yr. The fixed cost is due to the equipment needed for enclosures, a conveyor and the ball mill. The annualized fixed cost for the system is evaluated from data available in the literature (Peters and Timmerhaus, 1991) to be \$181,720/yr. By combining the operating cost along with annualized fixed cost, one obtains the total annualized cost of cryogenic shredding to be \$0.14/tire.

Lastly, the method of shredding via water jets is examined. Water jets are created by transforming the convertible potential energy of the high pressure water into kinetic energy by passing it through a small orifice (Yeaple, 1990). The high pressure is normally generated by a hydraulic-driven, double acting reciprocating pump known as an intensifier. The jets cut cleanly, do not create dust or heat, and do

not require resharping as with mechanical shredding. Also while saws only feature one-directional cutting, water-jets are able to cut multi-directional. Jets with pressures reaching 60 kpsi can even cut through steel (one-inch) at a rate of eight inches per minute (Raia, 1985). The proposed system is fabricated based on recent technology in water-jet shredding which provides a means of producing shredded rubber from scrap tires (Rutherford, 1992). This high pressure technology features separation of the steel cords in the carcass and the beading from the shredded rubber. The idea of this option is to basically strip the rubber from the steel cords yielding rubber in a sufficiently small size for use in other applications without further processing. In addition, steel is left in a fashion that allows it to be easily separated and sold as scrap metal. Of course several scenarios can prevail with respect to the number of nozzles/groups of jets and whether the jets are on the top or bottom. An example of one scenario is presented in Figure 3. The empirical equation used for designing this system is reported in U. S. Patent 5,115,983 (Rutherford, 1992) which can be described as follows:

$$\alpha = \frac{\text{pressure (kpsi)} \times \text{dwell time (sec.)} \times \text{flowrate (gal/min)}}{\text{impacted area (sq. in.)}} \quad (1)$$

It has been proven that for single-pass shredding, α ranging from 10 to 20 provides good stripping of all rubber leaving virtually bare steel (U. S. Patent 5,115,983). The units of water pressure, "kpsi", is defined to be 1000 psi. The patented process typically features rubber stripping employing water pressure ranging between six to 10 kpsi. Above 6 kpsi, one runs the risk of shredding the cord belts along with the rubber. The preliminary design proposed for this plant features water-jets at 8 kpsi with a defined dwell time of 10 seconds which is conservatively assumed to impact

only 25% of the available tire area per water-jet group. Hence, four water-jet groups are used. An average α value of 15 was chosen. Thus, Eq. (1) indicates that a flowrate of 75 gallons per minute of water are needed. Allowing five seconds spacing between each set of nozzles means that one tire will be shredded every 15 seconds at steady-state. The operating cost is due to conveying the tires (assuming a 30 ft. conveyor) and fixed cost is due to the cost of the conveying system and plunger pump yielding a total cost for water-jet shredding to be \$0.12/tire. By comparing the cost of the three shredding technologies, water-jet shredding should be selected.

5.3. Operating Cost

Raw materials cost is an important element of the operating cost. This plant utilizes 6250 lb/hr of coal which will cost \$561,188/yr based on an annual operation of 8760 hours per annum and \$20.5/ton of coal. On the other hand, scrap tires have a negative raw material cost (i.e., provide income) based on the tipping fee that is placed on all incoming scrap tires. This issue will be discussed later. One of the other contributors to the total production cost is the utility cost which partly entails the cost of heating/cooling in the plant. Indeed, the heating/cooling utility cost for this plant is due to heating/cooling that can not be achieved by integration of process. Hence, the total external heating and cooling utility needed is \$58,420/yr and \$8,440/yr, respectively. In addition, the cost of cryogenic cooling, needed for hydrogen separation and for cooling the naphtha flash column, is 602,587/yr. The operating labor cost is also a part of the operating cost and should be based on the annual capacity of the plant along with the number of processing steps. Thirty employee hours per day per process step are required (Peters and Timmerhaus, 1991) based on the product yield and an estimate of three processing steps (preparation, reaction, and

product recovery) in the plant. This results in an annual labor cost of \$492,750/yr based on average employee wages of \$15/hr. The other contributor to total utility cost is power primarily needed for shredding, crushing and pumping. The cost of electric power is taken to be \$0.08/kW-hr. The power needed for shredding is essentially due to the conveyor belts and pumping of water jets which cost \$291,762/yr to run. The power used for the coal crusher in coal preparation is approximately 30 hp (Corey, 1984) and results in an annual power consumption of 196,224 kWh/yr which cost \$15,698/yr in utilities. The power required for slurry pumping and compression of hydrogen from the hydrogen generation unit are 748,980 and 525,235 kWh/yr, whose annual costs are \$59,906 and \$42,012 per year, respectively. The cost of mass-separating agents needed for desulfurization is \$690,664/yr. Therefore, the annual operating cost (excluding depreciation) is \$2,823,427/year. By using a 10-year straight-line depreciation scheme, one obtains an annual operating cost (including depreciation) of \$14,699,527/year.

5.4. Annual Sales

Annual revenue is achieved by the sales of naphtha, light, middle, and heavy distillates, sulfur, scrap steel, and fuel gas. In addition, revenue can be achieved via the tipping fees for collecting scrap tires. The price of naphtha is taken to be \$0.79/gal (U.S. DOE, 1992). For conservative measures, the revenue projected to be obtained from the distillate fractions was calculated using the selling price of gas oil for the bulk distillate vapor fraction of the gas oil flash column. The resulting revenue is \$5,150,262/year. The sales of the fuel gases can be determined using the heating value of these gases along with the average dollar value per Btu (assumed to be \$3/Btu). Therefore, the annual value of fuel gases is \$329,853/year. Annual sales of

sulfur based on 99.5% recovery in the Claus unit is \$80,710/yr. The revenue from recovered scrap metal based on the price of scrap steel of \$105/ton is \$191,778/year. Hence, total annual revenue (excluding tipping fees for scrap tires) is \$5,752,603/year.

5.5. Break-Even Analysis

The break-even analysis is essential in this study. The purpose of this analysis is to show the point of operation of the processing plant at which the total production costs equal the total revenue generated. In this study, the break-even concept is used to determine the minimum tipping fee needed to be charged for collecting scrap tires to break even. This tipping fee is denoted by the symbol β , \$/tire. By equating the annual production cost \$14,669,527 with the annual profit (excluding tires) \$5,752,603 and the annual income from collecting scrap tires, the following equality is formed:

$$14,669,527 = 5,752,603 + 3,650,000*\beta \quad (2)$$

$$\beta = \$2.44/\text{tire} \quad (3)$$

This fee is relatively close to charges for disposal of used tires that have been recently reported to be as high as \$1.50/tire (U.S. EPA, 1991).

Since the primary objective of the co-liquefaction plant is to produce liquid fuels which will be ultimately compared to those derived from petroleum resources, another way of employing the break-even analysis is to incorporate a relative factor between these two technologies. First, this calculation will be based on a defined tipping fee of \$1.5/tire. Next, the total annual revenue is calculated using tires, sulfur, and steel which comes to be \$5,747,488/yr. This annual rate is summed with the lumped price increase that oil will have to undergo in order to break even. The current price of oil is taken to be \$18/bbl. Let γ be the ratio of the future oil price

needed to break even to the present oil price. The break-even point is determined from the following equation:

$$5,747,488 + 5,480,115*\gamma = 14,669,527 \quad (3)$$

$$\gamma = 1.63 \quad (4)$$

Therefore, the price of oil has to increase by 63% of its value today in order for this plant to break even. Figure 3 is a plot showing the conditions of oil price and scrap-tire collection fee under which the plant breaks even.

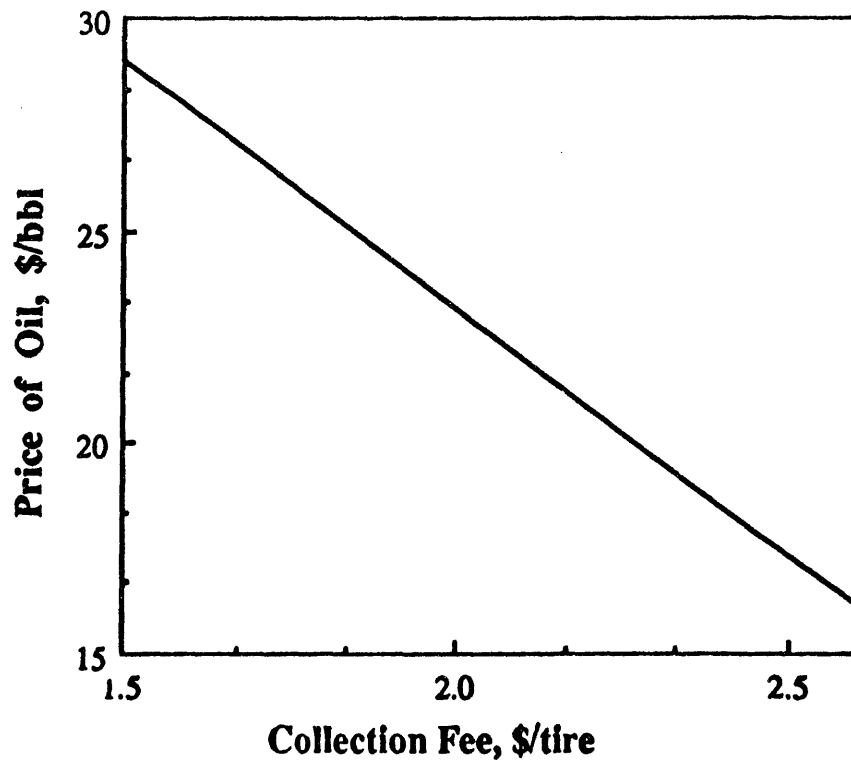


Figure 3. Conditions for Oil Price and Scrap Tire Tipping Fee Needed to Break Even

5.6. Return on Investment

Another way of assessing the profitability of this plant is to consider the return on investment [ROI] which is usually defined in the following way:

$$\text{ROI} = \text{Annual Profit} / \text{Total Capital Investment} \quad (5)$$

A desirable ROI for most chemical processing plants is 20%. Again, by employing the two previous concepts of potential tipping fee (β) and the ratio of the future price of oil to its current price (γ), the following two equations can be derived:

$$.2 = (5,747,488 + 5,480,115*\gamma - 14,669,527) / 139,687,000 \quad (6)$$

$$\gamma = 6.73 \quad (7)$$

$$.2 = (3,650,000*x + 5,752,603 - 14,669,527) / 139,687,000 \quad (8)$$

$$\beta = 10.10 \quad (9)$$

A plot depicting this notion of varying price of oil versus charge of collecting tires to yield several ROI's is shown in Figure 4.

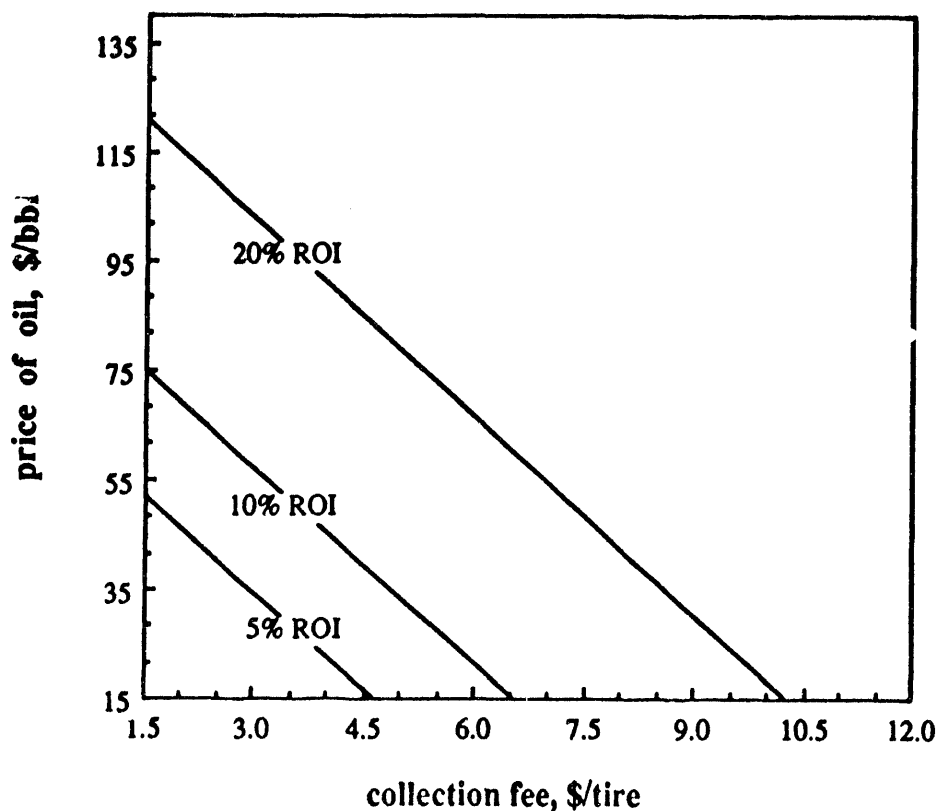


Figure 4. Effect of Oil Price And Tipping Fee of Tires on ROI

5.7. Comparison with Other Technologies for Utilizing Scrap Tires

It is also important to compare this co-processing plant to other existing tire conversion/processing technologies on an economic basis. The EPA (U. S. EPA,1991) suggested the use of the following definition of gross profit per tire:

$$\begin{aligned} \text{Gross Profit/tire} &= \text{tipping fee collected per tire} \\ &+ \text{revenue from tire products} \\ &- \text{facility operating cost per tire} \\ &- \text{transportation cost to bring in tires} \\ &- \text{disposal for waste products} \quad (10) \end{aligned}$$

The major limitation of this definition of profitability is that it excludes depreciation. Hence, one should also consider the notion of payback period to provide an indication of how long it takes to recover the capital investment of the plants where:

$$\text{Payback Period} = \frac{\text{Capital investment}}{\text{Gross annual profit (excluding depreciation)}} \quad (11)$$

The gross profit and payback period for plants utilizing scrap tires in power generation and cement-kilns combustion have been reported by the EPA (1991). These data along with results for the co-liquefaction of coal and scrap tires are summarized in Table 3. As can be inferred from this table, co-liquefaction provides a gross profit per tire that is higher than the two other technologies. This result is due to the high-value commodities produced by co-liquefaction. Nonetheless, co-

liquefaction requires longer payback periods than the two other technologies. This is attributed to the capital investment of the co-liquefaction plant which is significantly higher than that for power generation or cement kilns.

Table 3. Economic Comparison of Scrap-Tire Processing Technologies

Technology	Gross Profit \$/tire	Payback Period, yrs
Co-liquefaction with Coal	2.30	16.6
Power Plants:		
\$0.04/kW-hr	1.31	6.5
\$0.083/kW-hr	2.26	3.7
Combustion in Cement Kilns	0.75	1.4

6. CONCLUSIONS

This work has presented a technical and economic assessment of the co-liquefaction of coal and scrap tires. First, a conceptual flow diagram for the co-liquefaction plant was developed. Then, material balance was conducted for a plant co-liquefying 10,000 tires/day of scrap tires with an equal mass of coal. A plant-wide simulation was undertaken using ASPEN plus simulation package for preliminary sizing of the main pieces of equipment throughout the plant.

The economic assessment of this plant was undertaken. The fixed and working capital investments were found to be \$118,461,000 and \$139,687,000, respectively. By determining depreciation costs from these investment costs and calculating labor costs, utilities and the cost of raw materials, the total cost of co-liquefaction is \$14,669,527/yr. On the other hand, revenue is generated by the annual sales of useful products and by-products to recover \$1,769,489. Based on these findings, it was shown that in order for this plant to break even at current prices of \$18/bbl of crude oil, an average tipping fee of \$2.44/scrap tire must be collected. With this in mind, if this processing plant was looked upon as a waste-management facility for helping the nation with its growing problem of scrap tire disposal while producing useful transportation fuels, then this technology may be deemed feasible. Hence, an entity that has a vested interest in either helping clean up the environment or preserving our nation's steadily dwindling oil resources may initiate detailed design and further assessment of the conceptual processing plant presented in this paper. If it is desired to achieve an acceptable return on investment (5 - 20%) for the private sector, it is not recommended that this venture be undertaken without further research and/or a major increase in the current price of oil/tire.

Finally, co-liquefaction was compared with existing scrap-tire processing technologies. These technologies include combustion in power plants and cement kilns. It was found that co-liquefying scrap tires with coal provides a gross profit per tire that is higher than combustion. Nonetheless, due to the relatively high investment cost of co-liquefaction, it has a payback period that is much longer than combustion of scrap tires.

7. RECOMMENDATIONS AND FUTURE PLANS

In the future, more endeavors should be undertaken so as to enhance the conversion of coal in this co-liquefaction process. Further understanding of the chemistry involved and factors affecting the conversion is needed. For example, the effect of using liquefaction catalysts and varying operating conditions should be explored. The alternative of depolymerizing the scrap tires instead of using a recycled hydrogen-donor solvent should be examined. This proposition can lead to substantial reduction in the size of several pieces of equipment (e.g. pump, slurry mixer, reactor, etc.) and consequently significant cost savings. The possibility of using a reactor system other than ebullated beds should be examined. This aspect is particularly important in light of the high cost of the liquefaction system. Furthermore, the carbon black-rich stream "ash concentrate" should be characterized to identify any potential for revenue. If so, a means of separation carbon black before hydrogen generation should be devised.

Future plans include the refining of the current work by incorporating any new experimental data on the the co-liquefaction of coal and scrap tires. In this context, the current endeavors of the Consortium for Fossil Fuel Liquefaction Science can be instrumental. In addition, a similar approach will be adopted to investigate the feasibility of co-liquefying coal with other polymeric wastes and cellulosic materials.

8. BIBLIOGRAPHY

Farcasiu, M., 1993, "Another Use for Old Tires", Chemtech, January ,22.

Farcasiu, M. and C. Smith, 1992, "Coproprocessing Coal and Waste Rubber", Preprints of Papers, ACS National Meeting, San Francisco, Vol. 37, No. 1.

Farcasiu, M. and C. Smith., 1991, "Methods for Co-processing Waste Rubber and Carbonaceous Material", US Patent 5 061 363.

Jost, K., 1992, "Tire Materials and Construction", Automotive Engineering, October, 23-8.

Linnhoff, B. and E. Hindmarsh, 1983, "The Pinch Design Methods for Heat-Exchanger Networks", Chem. Eng. Sci., 38, pp. 745-763

Moore, D. and C. Aten, 1987, "Method and Apparatus For Treating Waste Products to Recover Components Thereof", US Patent 4 813 614.

Perry, R., 1993, "Give Us Your Poor, Huddled, Tire Masses", Chemical Engineering, February, 23.

Peters, M. and K. Timmerhaus, 1991, "Plant Design and Economics for Chemical Engineers, 4th ed., Chemical Engineering Series.

Raia, E., 1985, "Cold Cuts", Industrial Technology, December, 58-9.

Rutherford, D., 1992, "Process for Recycling Vehicle Tires", US Patent 5 115 983.

Snow, R. H., B. H. Kaye, C. E. Capes and G. C. Sresty, 1984, "Size Reduction and Size Enlargement", Perry's Chemical Engineer's Handbook, 6th ed., McGraw-Hill Book Company.

U.S. DOE, 1992, "Petroleum Marketing Monthly", Eng. Inf. Admin., Washington, D.C., DOE/EIA-030, August.

U.S. DOE Pittsburgh Energy Technology Center [PETC], 1993, "Direct Liquefaction Baseline Design and System Analysis", Final Report on Baseline and Improved Baseline, vol. IIA, March.

U.S. EPA, 1991, "Markets for Scrap Tires", EPA/530-SW-90-047B

Yeaple, F., 1990, "Growth Spurt for Water Jets", Design News, July, 77.

TITLE: CHEMISTRY OF CATALYTIC COAL LIQUEFACTION

PI(Authors): B. Bockrath, E. Illig, M. Keller, III, K. Schroeder, E. Bittner, J. Solar.

Institution/Organization: Pittsburgh Energy Technology Center

Period of Performance: 1993

Objective: The overall objective is to improve the scientific basis for using dispersed catalysts in the first stage of direct liquefaction processes. Three separate tasks are being pursued. The first concerns the preparation, use, and evaluation of dispersed catalysts under low-severity conditions. A pulse-flow microreactor is used to investigate hydrogen transfer reactions between catalyst and coal in the second task. In the third task, a micro-flow reactor consisting of a packed column in a gas chromatograph is developed, then used to determine the activity and selectivity of the liquefaction residues that contain dispersed catalysts.

Accomplishments and Conclusions: In this paper, emphasis will be placed on the accomplishments and conclusions arising out of the first task, that dealing with the preparation and evaluation of dispersed MoS_2 . A summary of results of the other two tasks is given for the sake of an overview. Experimental details may be found in the references cited.

Investigation of transport of hydrogen between catalyst and coal was the object of the second task. A pulse-flow microreactor was used for this purpose and related catalytic problems¹. The reactor was a simple quartz tube packed with physical mixtures of coal and catalyst. Pulses of hydrogen or deuterium gas were carried through the reactor by a stream of argon, and the gas stream was sampled at the exit by a capillary tube attached to the inlet of a quadupole mass spectrometer. The exchange reaction was found to be catalyzed by MoS_2 when the reactor was packed with a physical mixture of the coal and catalyst². A limited amount of the hydrogen in coal participated in the exchange, which could be observed with MoS_2 at temperatures as low as 200° C, and even lower with a Pd on carbon catalyst³. A speculative rationale has been developed based on the results of a series of experiments with different catalysts and exchange substrates. It is presumed that hydrogen gas dissociates on the surface of the catalyst and then may exchange with a certain pool of hydrogen in the coal made accessible by transport over a network of hydrogen-bonded phenols. Thus, activated hydrogen has rapid access to the interior of coal particles by means of a series of chain transfer steps. In this view, hydrogen mobility is distinguished from molecular mobility, the former being much more rapid than the later in the case of coal heated in the absence of a solvent. These results point to the possibility that a prime role of catalyst in the conversion of coal is that of a termination site for free radical chain reactions that may originate within the interior of coal particles.

Testing dispersed catalysts is a generic problem that may

always benefit from still better approaches. An approach taken up under the third task of this project is the determination of catalyst activity and selectivity using model compounds in the vapor phase. A micro-flow reactor has been developed by using the basic components of a gas chromatograph. Thus, solutions containing the model compounds are injected into a stream of hydrogen and passed through a stainless steel column packed with dispersed catalyst. The column is housed in the oven of the chromatograph, which provides excellent temperature control. The reaction products are collected at the exit port of a thermal conductivity detector and analyzed by gas chromatography. Alternatively, an HPLC pump has been used to deliver solutions of model compounds to the injection port at a constant rate. Operation in this continuous mode allows steady state conditions to be approached. Preliminary results have shown that the dispersed catalysts prepared using massive loading of the catalyst precursor as described below are active in hydrodesulfurization reactions at low temperatures (350° C) and low hydrogen pressures (~3 atm). Other work under this task sprang from the recognition that the dispersion of the catalyst precursor achieved on the coal prior to liquefaction may have an effect on the character of the catalyst eventually formed. Thus, a study was begun to explore the effect of pH on the extent of molybdate adsorption and its degree of dispersion. Control of the solution pH and the initial molybdate concentration allows adjustment of both the surface properties of the coal and the molybdate chemistry. The results indicate that the amount adsorbed is indeed a function of the pH and of the molybdate concentration of the solution⁴. Work in progress is designed to determine the effect of the parameters of precursor deposition on catalyst performance.

The prime subject of this report is a series of microautoclave experiments carried out to explore the factors that affect the performance of dispersed MoS₂ catalysts. In this work, an approach for evaluating catalyst performance developed in a study⁵ of the low temperature liquefaction of Illinois No. 6 coal has been adopted. Catalysts are prepared by impregnating a precursor on the coal and subjecting the treated coal to liquefaction conditions in a microautoclave. After liquefaction, the catalyst is recovered by extracting the liquid product with tetrahydrofuran (THF). The insoluble portion is weighed after being dried in a vacuum oven. The required portion of this residue is then charged to a microautoclave with fresh feed slurry and subjected to liquefaction conditions. Catalyst performance is then judged according to the relative amount of coal conversion determined by sequential extraction with cyclohexane and THF, and by the pressure drop over the course of the reaction that is recorded by means of a pressure transducer.

The details of this process may be illustrated by discussion of a typical experiment. A 3.3 g (3.0 g maf) sample of DECS-17 coal was used as received from the DOE sample bank at The Pennsylvania State University. This sample is a high volatile bituminous (hvbC) Blind Canyon, Utah coal. The dry, ash-free elemental analysis was C= 81.6%, H=6.2%, N=1.4%, O=10.4%, and S=0.4%. The dry pyritic sulfur was 0.02%. As-received moisture and

ash were 3.7% and 6.3%, respectively. The coal had been ground to pass 60 mesh. Application of $(\text{NH}_4)_6\text{Mo}_7\text{O}_{24}$ to the coal was accomplished by mixing with a ~0.1 molar solution of the precursor. An amount of this solution was used to provide a catalyst loading of 100,000 ppm Mo (10%) based on the dry weight of the coal. The coal was then dried overnight in a vacuum oven at 60° C.

The catalyst preparation step was carried out in small batch microautoclaves described previously⁶. Briefly, these autoclaves were of about 42 mL capacity and equipped with a pressure transducer and an internal thermocouple. A set of six autoclaves was mounted on a single shaker unit and heated in a fluidized sand bath. The reactors were shaken at about 60 cpm in a motion that followed an arc with the highest point at the center of its path. A slow heat-up procedure, which was used in all of this work, was performed by turning on the sandbath heaters after the autoclaves were immersed in the cold sandbath. The nominal reaction temperature, 375° C, was reached in about 60 min. The autoclaves were held at this temperature for 120 min, then cooled rapidly by immersion in another fluidized sand bath held at room temperature.

In addition to the coal, the autoclave was charged with 6.0 g of a coal-derived hydrotreated distillate (V-178) obtained from operations at the Advanced Coal Liquefaction R & D Facility at Wilsonville, Alabama. The carbon and hydrogen contents were 88.2% and 9.6%, respectively. By D-1160 distillation, 84% distilled below 850° F. Sufficient hydrogen was charged to bring the total pressure to about 2000 psig at operating temperature. Often, the hydrogen charge contained 3% H₂S. In some cases, additional sulfur was provided by the addition of either CS₂ or elemental sulfur.

Workup of the samples was accomplished by solvent extraction. First, the reactors were depressurized and a gas sample taken for analysis by gas chromatography. Coal conversions were calculated on an maf basis from weights of residues dried in a vacuum oven after vacuum filtration on 8μ paper, first using cyclohexane, then THF.

Evaluation of catalyst performance was accomplished in a separate liquefaction cycle by taking a portion of the dried liquefaction residue and adding it to a fresh charge of coal and liquefaction solvent in the autoclave. The residue was quite friable and was ground in a mortar to roughly 60 mesh before it was used. An amount of residue was added to make a charge of 2000 ppm Mo on dry weight of fresh coal. The coal and liquefaction solvent were used in the same portions as in the preparation step. The autoclave was charged with hydrogen/H₂S and the same heating cycle was repeated. Product workup was then carried out as before.

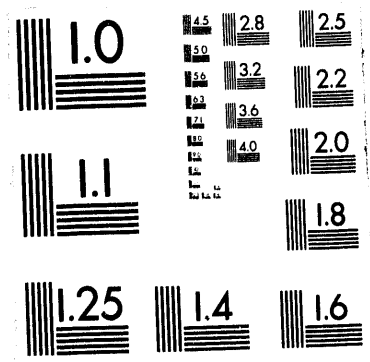
The decision to use a two-step preparation/evaluation program was based on several considerations. In general, the evaluation of dispersed liquefaction catalysts presents a number of difficulties. Some of these difficulties may arise when the catalyst is introduced to the reactor in the form of a precursor. In a one-step screening test, the conversion of precursor to catalyst takes place during the initial time span of liquefaction. Thus, the character of the material being formed undergoes considerable change during the time when important liquefaction reactions take place. Under these conditions, the ability of the catalyst to

influence the initial stage of liquefaction becomes dependent on many external factors, including the heating rate, hydrogen pressure, sulfur content in the reactor, character of the precursor, and the means chosen to disperse it. Thus, the performance achieved in a one step test may well depend on factors other than the properties of the catalyst eventually formed. A two-cycle program allows separate evaluation of the factors that influence the generation of the catalyst and the performance of that catalyst during the entire course of the liquefaction reaction.

In addition to improved catalyst screening, certain advantages may be seen in this approach from the processing point of view. Impregnation of coal with precursors is an added burden on the overall cost of the liquefaction process. An advantage of a separate stage for catalyst preparation is that the need to impregnate all of the coal is avoided. Impregnation of a small fraction may suffice. Further, if the catalyst is prepared in a separate reactor, the conditions may be adjusted to optimize the quality of the catalyst rather than being dictated by the conditions necessary for coal conversion. The most appropriate organic feedstock for use in generating catalyst is not necessarily the same feed coal used in the process, but could be other coals. Even different feed streams could be introduced into the liquefaction process in this way. A tailor-made and fully activated catalyst made under optimum conditions could be introduced to the main liquefaction reactor where full advantage could be extracted from it under conditions optimized for catalytic liquefaction.

The influence of added molybdenum on the total pressure within the reactor during the catalyst preparation step is illustrated in Fig. 1. A large difference in the change in total pressure with time is seen between the reactors with and without molybdenum. In this illustration, CS_2 has been added to provide sufficient sulfur to complete the sulfidation of the relatively large amount of catalyst precursor added. The deviation between the two pressure curves begins at about $240^\circ C$. A portion of the difference is due to the net consumption of gas in the production of H_2S from CS_2 . However, it is still clear that hydrogenation activity begins well before the nominal reaction temperature, $375^\circ C$, is reached. The amount of hydrogen taken up is considerably larger by the end of the reaction for the catalytic reaction. The THF conversions, 91% without and 92% with catalyst, were near the maximum expected for this coal, which contains 8.2% inertinite. However, the cyclohexane conversion was 41% with catalyst, considerably higher than the value of 21% achieved without catalyst.

The results obtained when the prepared catalyst was reused at 2000 ppm on fresh coal are illustrated in Fig. 2. The change in total pressure may again be compared with that found without catalyst or that with 10% Mo used in its preparation. Examination of the numerical values of the pressure data recorded during the reactions reveals that both catalytic curves begin to deviate from the uncatalyzed case in the temperature range of 220 to $250^\circ C$. This may well represent the onset of thermal reactions that may use hydrogen from the catalyst surface. The amount and rate of



2 of 8

hydrogen consumption is larger using the liquefaction residue than the uncatalyzed case, but not as large as is found with the massive loading used to prepare catalyst. The THF conversion was 91%, again near maximum, but the cyclohexane conversion was 27%, a value between that for 10% Mo and the uncatalyzed reaction. The results show the approach is a practical way of making catalyst. The target for further research must be to increase catalyst activity so that higher conversions may be obtained without resorting to impractical amounts of catalyst.

Comparison of the change in gas pressure given above leads to the question of whether the amount of catalysts present is the sole factor governing the amount of hydrogen used. A set of three experiments was conducted in which the amount of coal added was increased in steps from 0 to 3 to 5 g, but the amount of catalyst added was held constant at what would be used to make the typical charge of 2000 ppm Mo on 3 g maf coal. As may be seen in Fig. 3, the amount of hydrogen taken up is proportional to the amount of coal in the reactor. Without coal, the liquefaction solvent by itself took up only a small amount, as would be expected for a hydrotreated liquid. The THF conversions were 96% and 94% for the coal loadings of 3 g and 5 g, respectively. Cyclohexane conversions were 31% and 28%, respectively. These data indicate that provided more than a certain minimum amount of catalyst has been added, the hydrogen uptake depends mainly on the amount of coal present. The demand for hydrogen placed upon the catalyst at this point in the liquefaction sequence arises from thermal reactions initiated in the coal.

The shapes of the pressure/time curves are also of interest. The amount of gas produced is dependent on the quantity of coal in the reactor. The high point in pressure is reached within the first minutes after the reactor temperature reaches its plateau. This again confirms that the majority of the gas evolved from the coal appears within minutes of reaching reaction temperature. After the high point is passed, the initial rates of pressure drop may be compared for the three cases. In this comparison, the pressure drop in psig per min was calculated for selected time intervals, and the ideal gas law applied to approximate the net mols consumed per gram of coal per min. The drop due to liquefaction solvent is small and may be factored out by subtraction of its rate corrected for the amount of solvent in the remaining two cases. When this was done, the rates during the interval from 10 to 20 min beyond reaching reaction temperature were identical, 0.055 mmol/min-g coal for the 3 and 5 g loadings. During the interval from 20 to 30 min beyond reaching reaction temperature, the rates were slightly less, 0.048 and 0.054 mmol/min-g coal, respectively. The close agreement between these crude estimates of rates supports the suggestion that the rate of hydrogen uptake is largely determined by the requirement exerted by coal thermolysis. In this view, a prime function of the catalyst is to act as a radical chain terminator by supplying hydrogen to free radicals. The concept of catalytic control of free radical reactions to promote the formation of oils and suppress the formation of coke has been described previously in connection with the use of MoS_2 ⁷.

The effect of total pressure on the rate of pressure drop was explored by comparison of reactions at nominal pressures of 2000 and 4000 psig. The results may be seen in Figure 4. In these experiments, the catalyst was again a liquefaction residue added at the level of 2000 ppm on fresh coal. It was prepared in the experiment illustrated in Fig. 1. The rate of pressure drop is dependent on total pressure. The rates for the interval from 10 to 20 minutes after reaching reaction temperature were derived as before. The values were 0.043 and 0.062 mmol/min-g coal for 2000 and 4000 psig, respectively. Coal conversions may also be compared. THF conversions were 91% in both cases, again near the maximum expected. The cyclohexane conversion at the higher pressure was 33%, slightly more than the value of 27% found at lower pressure.

A limited range of preparation variables has been surveyed to determine the effect of the preparation conditions on the performance of the catalyst obtained. The results of some of this work are summarized in Table 1. The evaluation conditions were the same in all cases, 2000 ppm of Mo on fresh coal, 3% H₂S in H₂ at 2000 psig at reaction temperature of 375° C. Baseline experiments without added catalyst are also included for comparison. Conversions with and without added catalyst are nearly the same, but the amount of hydrogen consumed in the absence of catalyst is significantly smaller. The presence of H₂S is important even in the absence of added catalyst, as may be seen by the reduction in the amount of hydrogen taken up when pure hydrogen rather than H₂/3% H₂S is charged without catalyst. The addition of catalyst under these conditions brings the THF conversions near the maximum. Cyclohexane conversions were far from the maximum, but quite similar in all cases. Under these reaction conditions, the main indication of catalytic activity is the amount of hydrogen consumed. The cyclohexane conversions provide a weak secondary indication.

Hydrogen uptake data have been included in Table 1 in two forms. The first is the pressure change observed across the time interval beginning from the moment the reactor reaches reaction temperature until it is removed from the heated sandbath. This change represents the sum of both gas consumption reactions and gas producing reactions. The latter include the production of CO₂, light hydrocarbon gases, and any steam arising from chemical reactions. The production of these gases is relatively small at this low temperature and accounts for about 5% of the total gas pressure by the end of the reaction. More importantly, the yield of gases from coal does not seem to be greatly affected by the presence of catalyst. Comparisons of total pressure decreases are thus meaningful in terms of relative trends in hydrogen uptake. Also given in Table 1 are values for hydrogen uptake expressed in mmols. These values are based on the change in total pressure between the time when the reactor is first charged until the reactor has reached room temperature again after the reaction. Gas samples were analyzed by gas chromatography, and the molar amounts of the coal-derived product gases were calculated. The amount of hydrogen taken up was then estimated using the ideal gas law. The trends within each set of data are consistent. The amount of

hydrogen taken up was in the range of 1.0 to 1.7 wt% of coal.

The catalysts were prepared at initial loadings ranging from 1 to 10%. Over this range, the loading seemed to have little effect on the subsequent performance of the catalyst. In one case, the coal-to-liquefaction solvent ratio was increased to 2/1 from the usual value of 1/2. Thus, twice as much catalyst was produced per reactor volume. The performance of this catalyst was adequate in terms of coal conversion, but in the lower range in the total amount of hydrogen taken up.

It may be noted that the lowest hydrogen uptake was found with one preparation at 10% loading of molybdenum. In this case, the only source of sulfur was the 3% of H₂S charged with the hydrogen. From the analysis of the product gases, it is evident that the amount of H₂S charged was nearly totally consumed. Insufficient sulfur to complete the sulfiding of the catalyst may then be a contributing factor to the lesser amount of hydrogen taken up when this catalyst was used in the subsequent liquefaction experiment.

The approach suggested here to separate the catalyst preparation from catalyst use permits two different feedstocks to be used. This is illustrated by the use of a Leonardite in the preparation step. The catalyst made by impregnation of 10% Mo on this low rank material generally performed as well as those made with Blind Canyon coal. This possibility opens a wide range of choice for catalyst preparation that we intend to explore further.

Summary.

The approach explored here in preliminary fashion suggests an alternate way dispersed catalyst might be integrated with a liquefaction process. The preparation of catalyst would be carried out in a special reactor resembling a first-stage liquefaction reactor but operated at conditions optimum for producing active catalyst. A small fraction, perhaps as little as 1% of the total liquefaction feed, would be impregnated with precursor. The conditions of temperature, hydrogen partial pressure, sulfur concentration, heat-up rate, residence time, and degree of mixing need to be established to provide optimum catalyst characteristics. The entire liquid product of this reactor would then be introduced to the main liquefaction reactor without intermediate separation. The liquefaction reaction would then be carried out under the optimum conditions for coal conversion. As always, the choice of feedstock for the main process would be based on the coal conversion characteristics. The material of choice for catalyst preparation could be based on what is most suitable for the formation of the optimum catalyst, and need not be the same coal, or even be a coal.

References.

- 1) E. W. Bittner; B. C. Bockrath; J. M. Solar, submitted, J. Catalysis.
- 2) B. C. Bockrath; D. H. Finseth; M. R. Hough, Fuel, 71, 767, (1992).
- 3) B. C. Bockrath; J. M. Solar; E. W. Bittner; M. R. Hough, Proceedings, 1991 International Conf. on Coal Science, 691,

- Butterworth-Heinemann, Oxford, (1991).
- 4) K. T. Schroeder; B. C. Bockrath; M. L. Tate, Am. Chem. Soc. Div. Fuel Chem., Preprints, 38(2), 512, 1993.
 - 5) B. C. Bockrath; E. G. Illig; M. J. Keller, III, Am. Chem. Soc. Div. Fuel Chem. Preprints, 37(1), 133, 1992.
 - 6) R. R. Anderson; B. C. Bockrath, Fuel, 63, 329, (1984).
 - 7) R. Bearden; C. L. Aldridge, Energy Progress, 1, 44, (1981).

Table 1. Evaluation of catalysts made under various conditions.

Mo, wt% as prepared	1	4	6	10	10 ^a	10 ^b	10 ^c		
Mo, ppm fresh coal	2000	2000	2000	2000	2000	2000	2000	0 ^d	0 ^e
THF conv. %	92	87	91	91	89	91	91	89	81
CHX conv. %	27	28	23	27	28	29	24	22	17
Press. Change ^f	365	320	300	314	267	289	333	194	115
Hydrog. Uptake ^g	25.5	22.3	20.1	21.6	15.9	22.0	25.9	14.6	13.4

a. Catalyst prepared with 3% H₂S without supplemental sulfur.

b. Solvent/coal = 1/2 instead of 2/1.

c. Leonardite substituted for Blind Canyon coal in preparation step.

d. Uncatalyzed reaction, average of 2 experiments.

e. Uncatalyzed reaction under H₂ without 3% H₂S.

f. Total drop in pressure over the 120 min time at 375° C reaction temperature, psig.

g. mmols hydrogen uptake based on pressure difference taken at room temperature, gas analyses, and ideal gas law.

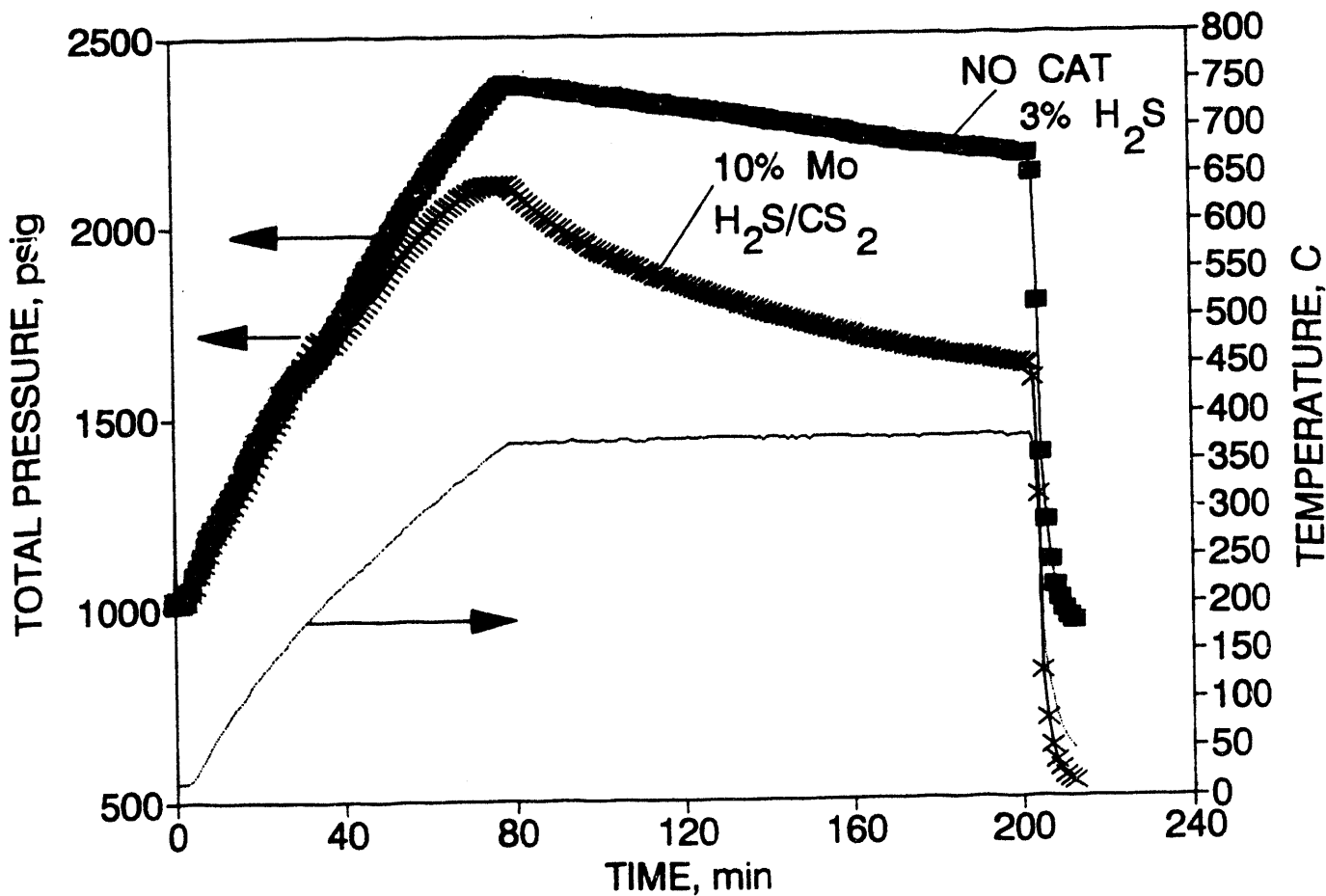


Figure 1. Total pressure and temperature within the microautoclaves as a function of time. The lower pressure curve corresponds to a sample of Blind Canyon coal that has 10 wt% Mo applied as $(\text{NH}_4)_6\text{Mo}_7\text{O}_{24}$.

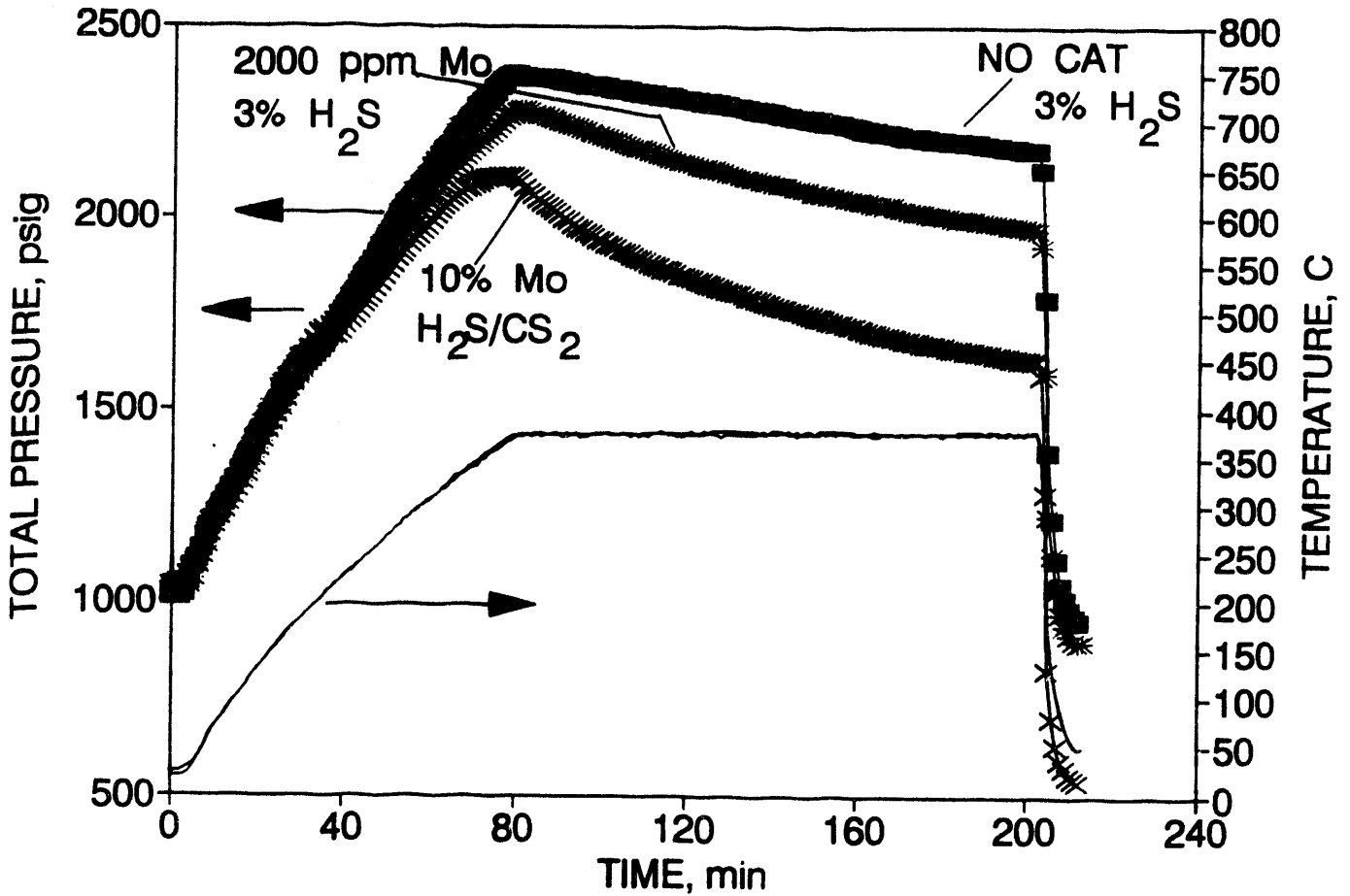


Figure 2. Total pressure and temperature within the microautoclaves as a function of time. The upper and lower pressure curves are the same as in Figure 1. The middle pressure curve corresponds to fresh Blind Canyon coal mixed with a fraction of the THF insoluble residue of the 10% Mo experiment that supplies 2000 ppm Mo.

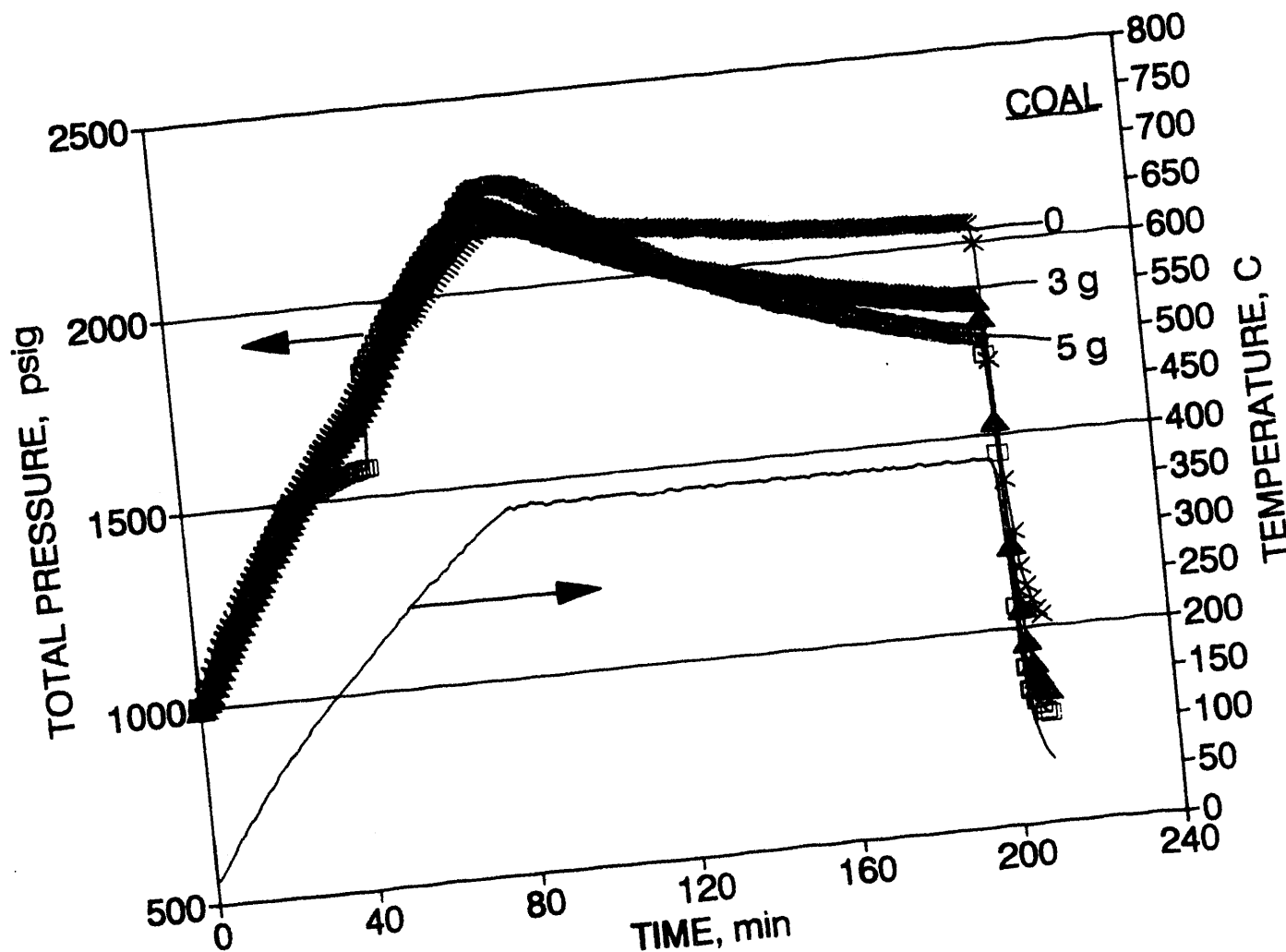


Figure 3. Total pressure and temperature within the microautoclaves as a function of time. The dependence of the pressure decrease on the amount of coal charged is evident. Each reactor was charged with the same amount of prepared catalyst. The loading was equivalent to 2000 ppm Mo on a 3 g coal charge.

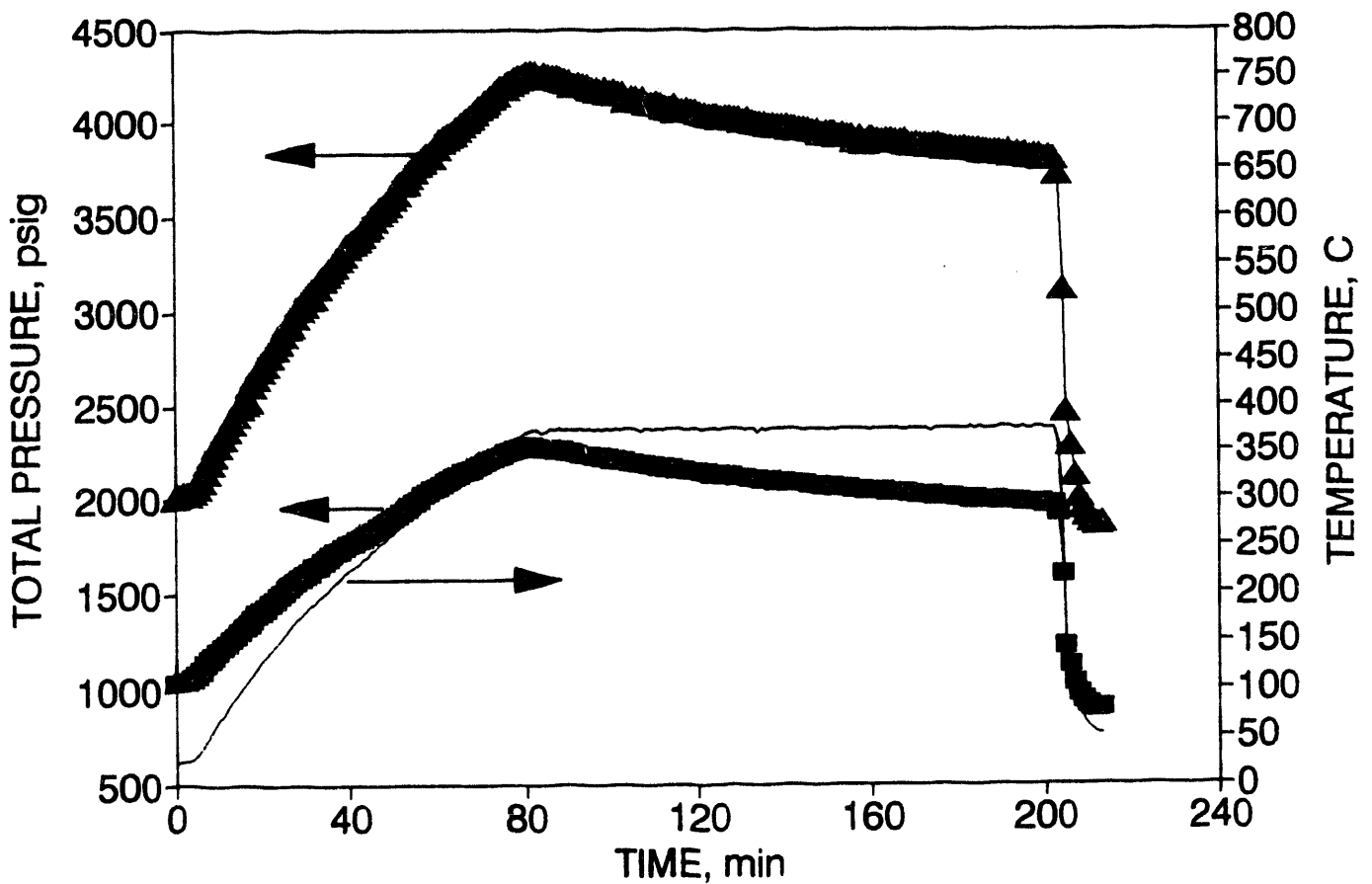
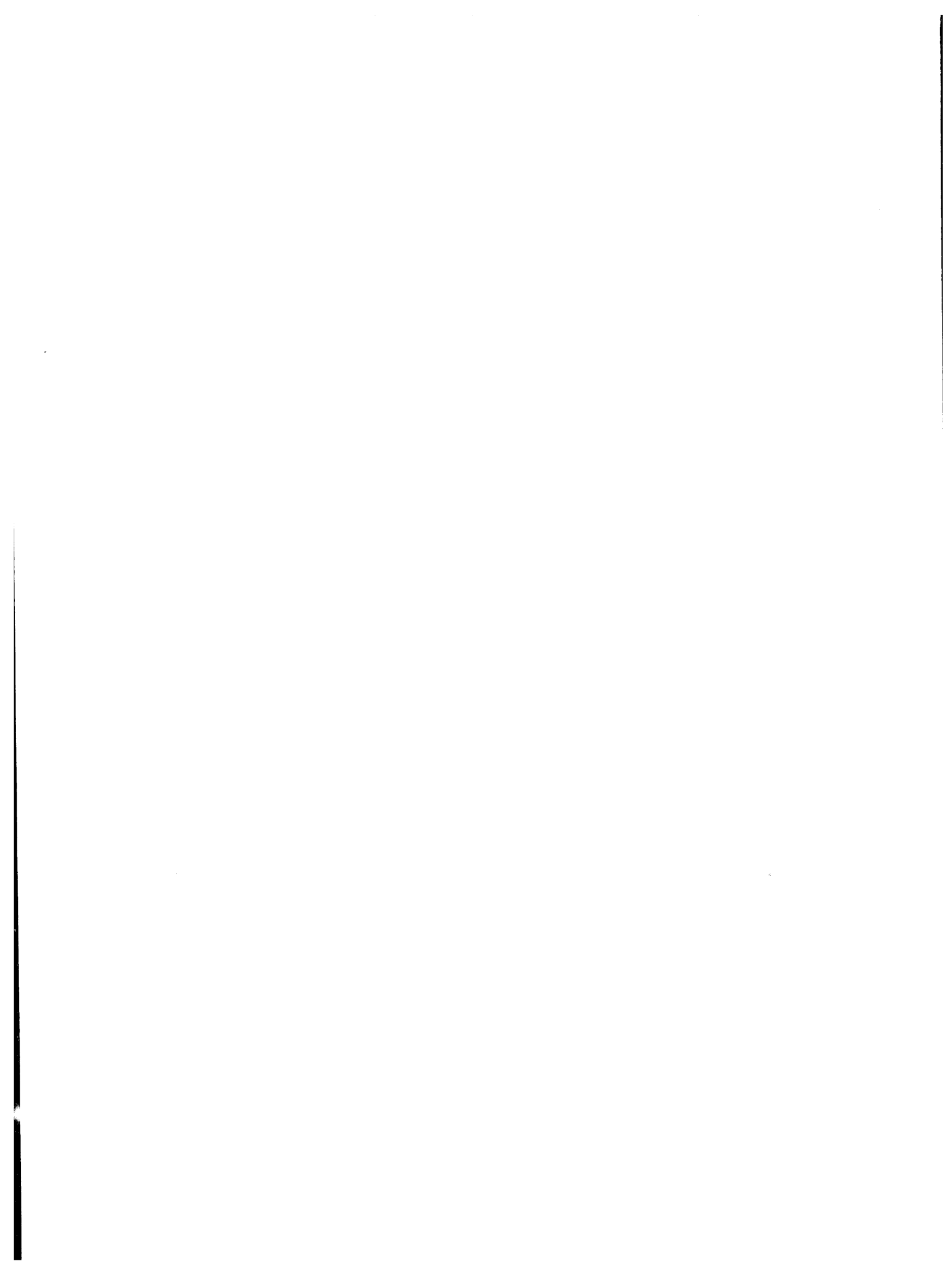


Figure 4. Total Pressure and temperature within the microautoclaves. The loading of prepared catalyst was 2000 ppm Mo based on fresh Blind Canyon coal. A greater rate of hydrogen uptake is evident at the higher pressure.



Title: HIGH TEMPERATURE/HIGH PRESSURE ESR SPECTROSCOPY OF FREE RADICALS IN COAL LIQUEFACTION, COPROCESSING AND CATALYST TESTING

PI's: M. S. Seehra and M. M. Ibrahim
Physics Department, P.O. Box 6315
West Virginia University, Morgantown, WV 26506

Contract No.: DE-FC22-90PC90029

Period of Performance: May 1, 1992 - June 30, 1993

Objectives:

The objectives of this project were to characterize Fe-based catalysts used in direct coal liquefaction research for their chemical nature and for particle size distribution, and to test these catalysts for direct coal liquefaction using recently developed in-situ high temperature/high pressure electron spin resonance (ESR) spectroscopy apparatus. Nine nanophase Fe_2O_3 and FeOOH based catalysts were investigated. Some experiments on the coprocessing of coal with waste tires and polymers have also been carried out.

Accomplishments and Conclusions:

Details of the high temperature/high pressure ESR cavity system for experiments at x-band (~9 GHz) frequencies have been given in recent papers [1,2]. With this system, experiments can be carried out from ambient to about 600°C in gaseous pressures up to 600 psi, and also in vacuum in an evacuated sealed ESR tube and in flowing gases. The intensity of the signal, measured by double integration of the standard derivative ESR signal, is normalized to a standard to yield the free radical density N , along with the measurements of the g -value and the linewidth ΔH . Complimentary thermogravimetric (TG) measurements were also carried out in many cases.

Nine Fe-based catalysts were obtained from Professor Wender of the University of Pittsburgh [3]. These are $\text{Fe}_2\text{O}_3/\text{SO}_4(1)$, $\text{Fe}_2\text{O}_3/\text{SO}_4(2)$, $\text{Mo}/\text{Fe}_2\text{O}_3/\text{SO}_4$, $\text{Fe}_2\text{O}_3/\text{SnO}_2/\text{SO}_4$, $\text{Fe}_2\text{O}_3/\text{MoO}_4$, $\text{Fe}_2\text{O}_3/\text{WO}_4$, FeOOH/SO_4 , $\text{Mo}/\text{FeOOH}/\text{SO}_4$, and Fe_7S_8 . The linebroadening of the x-ray diffraction lines [4] was used to determine the particle size of these catalysts. These sizes were found to be (in Å units): 110 ± 30 , 250 ± 35 , 140 ± 45 , 20 ± 5 , 140 ± 20 , 290 ± 35 , 75 ± 25 , 50 ± 20 , 400 ± 100 , in the order listed above [5]. All the experiments were carried out with Blind Canyon coal with the following loadings: $\text{Fe}/\text{coal} = 1/99$; $\text{Fe}/\text{S} = 1/2$. For testing of these catalysts, free radical density N was measured from room temperature to 500°C in flowing H_2 gas and these values were compared with the case of coal alone. In all cases, above about 350°C, N was found to be higher in the presence of the

catalysts, signifying hydrocracking by the catalysts. TG measurements were used for mass correction of the data.

To measure catalytic activity, we define $R = N_{\text{cat}}/N_{\text{coal}}$ at 400°C, where N_{cat} and N_{coal} are respectively the free radical densities with and without catalyst loadings. In the order of the catalysts listed above, we found the following R values for the various catalysts: 2.21, 1.15, 1.72, 2.31, 1.65, 2.45, 1.30, 1.10, 1.70. The difference between Fe₂O₃/SO₄(1) and Fe₂O₃/SO₄(2) may be due to the large particle size of Fe₂O₃/SO₄(2). In general, the Fe₂O₃-based catalysts have higher activity than the FeOOH-based catalysts. This result is in agreement with the results obtained by direct liquefaction experiments [3,6]. Thus these experiments have demonstrated that in-situ ESR provides an excellent method for testing catalyst efficiencies for direct coal liquefaction [5]. In a recent paper [7], the same technique has been applied to demonstrate that waste tires promote enhanced coal liquefaction.

Plans:

Recently, we have developed a new approach to in-situ ESR spectroscopy in which catalysts can be introduced to a coal sample maintained at a high temperature (e.g. 400°C) followed by monitoring of the free radical signal. This approach has confirmed the hydrocracking ability of Fe₂O₃/SnO₂/SO₄. In the near future, similar experiments with the other catalysts, waste-tire components and polymers will be carried out. Plans are also underway to extend the high pressure capabilities beyond 600 psi using sapphire tubes.

References:

1. M. M. Ibrahim and M. S. Seehra, Am. Chem. Soc. Div. Fuel Chem. Preprints, 37, 1131 (1992); *ibid* 38, 180 (1993).
2. M. M. Ibrahim and M. S. Seehra, Energy & Fuels, 5, 74 (1991).
3. V. R. Pradhan, J. W. Tierney, I. Wender and G. P. Huffman, Energy & Fuels, 5, 497 (1991).
4. M. M. Ibrahim, J. Zhao, M. S. Seehra, J. Mater. Res. 7, 1856 (1992).
5. M. M. Ibrahim and M. S. Seehra, Energy & Fuels (in press).
6. V. R. Pradhan, J. Hu, J. W. Tierney, and I. Wender, Energy & Fuels 7, 446 (1993).
7. M. M. Ibrahim and M. S. Seehra, Am. Chem. Soc. Div. Fuel Chem. Preprints 38, 841 (1993).

SYNTHESIS AND CHARACTERIZATION OF NOVEL IRON-BASED CATALYSTS FOR DIRECT COAL LIQUEFACTION

M. Mehdi Taghiei, J. Zhao, Z. Feng, K.R.P.M. Rao, F. E. Huggins,
and Gerald P. Huffman

233 IMMR, University of Kentucky, Lexington KY, 40506

Introduction

Catalyst particle size has a strong effect on catalytic activity and selectivity during direct coal liquefaction. Fine particles are desirable because the majority of the atoms are coordinatively unsaturated and have a large percentage of surface sites that are readily accessible for chemisorption and catalysis. Ion-exchange procedure plays a very important role in many chemical processes, because of its simplicity, selectivity, and finally its wide scope. Ion-exchange in which an ion in coal such as calcium is replaced by a catalytic ion such as iron can yield an ultrafine particle size with an even distribution of catalytic ions. This constitutes a new class of catalyst stabilized in a state of high dispersion even at coal liquefaction conditions. The work during this period focused on investigation into the role of ion-exchanged iron during direct coal liquefaction (DCL) of two lignites and a subbituminous coal. The results indicate that iron ion-exchanged into the low-rank coals constitutes a catalyst in a state of dispersion ranging from molecular ions to particles a few nanometers in diameter^{1, 2}. On the other hand, highly dispersed ferrihydrite catalysts have been synthesized with simple precipitation methods. The average particle sizes of these catalysts are less than 100Å. By doping a second component in the iron oxide

catalyst, a binary system can be formed. The particles of the binary Si-ferrihydrite and Al-ferrihydrite catalysts exhibit no agglomeration at temperatures up to 400°C. Results of direct coal liquefaction tests indicate that these catalysts are more effective than commercially available iron catalysts.

I. LIQUEFACTION OF LOW-RANK COAL CONTAINING CATION-EXCHANGED IRON

The coals used in this study are Beulah lignite (obtained from Department of Energy Coal Samples, DECS-11) and Hagel lignite (obtained from Penn. State Office of Coal, PSOC-1482) from the Fort Union region in North Dakota, and a subbituminous Black Thunder coal. The original iron contents of these coals are less than 0.5 percent. The coal samples were first ground to <200 mesh under a nitrogen atmosphere. The ion-exchange experiments were carried out in a 10 liter fermenter equipped with temperature and pH controllers. A freshly made 0.05M aqueous solution of ferric acetate was kept at a controlled pH of about 2.8 using sulfuric acid and a constant temperature of 333K. A slurry made from a 10:1 ratio by weight of dry coal to ferric acetate was stirred under a nitrogen atmosphere for 20 hrs. At the completion of the procedure, the ion-exchanged coals were repeatedly washed with distilled water until the pH value of the filtrate for two consecutive washes was constant. The iron contents of the Beulah and Hagel lignites and Black Thunder coal after the ion-exchange process were 7.8%, 5.33%, and 3.8%, respectively. The efficiency of lower loadings of iron in the ion-exchanged coals during liquefaction was

also investigated; samples of the same lignites were first demineralized in a manner similar to the procedure described by Bishop and Ward³ and then ion-exchanged to final iron contents of 0.93% for Beulah, and 0.88% for Hagel lignite.

Liquefaction Experiments

Two sets of coal liquefaction experiments were conducted. The first set of experiments was carried out with tubing bombs in a fluidized sand bath. This set of experiments was designed to investigate the effect of ion-exchanged iron catalysts on the total yield and product distribution in the liquefaction process. Control liquefaction experiments, using slurry mixtures of the same coal samples with a 30Å iron oxide (ferrihydrite) and with no catalyst, were run under the same conditions. The second set of experiments was designed to generate larger samples for the detailed characterization of the chemical structure and reactions of the added iron. The apparatus used to prepare the samples for these experiments was a one liter autoclave. This autoclave was connected at the top to a vessel for holding the sample prior to heating. At the bottom, four nitrogen-purged sampling lines were attached to the outlet valve of the autoclave to collect the liquefaction products directly from the autoclave without exposure to air. Liquefaction experiments were performed in the presence of excess tetralin and dimethyl disulfide (DMDS) as a sulfur donating species.

Mössbauer and XAFS Spectroscopy

Mössbauer spectra for the as-received, demineralized, and ion-exchanged coal samples were obtained using a conventional constant-acceleration-type Mössbauer spectrometer⁴. Calculation of the particle size distribution is described in detail

elsewhere⁵. XAFS measurements were performed at beam line X-19A at the National Synchrotron Light Source in Brookhaven National Laboratory. Iron K-edge XAFS spectra of the samples were obtained in transmission mode using a Si(111) double crystal monochromator.

Results and Discussion

The total conversion and product distribution of oils, asphaltenes, and preasphaltenes for Beulah, Hagel lignites, and Black Thunder coal from the tubing bomb liquefaction experiments at 673K for 60min are illustrated in Figure 1(a, b, and c). It can be seen that the asphaltene and oil conversion yields increased significantly for all ion-exchanged coals, with a sulfur donating species (DMDS) present. The preasphaltene yields, however, tend to decrease as a result of iron species incorporated into the coal. The variation in the product yields with the addition of a catalyst may be related to the conversion of preasphaltene and asphaltene as the reaction proceeds. It is evident from Figure 1 that the ion-exchanged iron is a more active catalyst than the 30Å ferrihydrite. Both the total conversion and the oil yield are substantially greater for the ion-exchanged iron than the 30Å catalyst at approximately the same concentrations. Elemental analyses of all three coals before and after the ion-exchange process indicate that the calcium content of these samples decreased by about 1.2% after treatment, while the concentration of other alkali and alkaline earth cations remains more or less constant. Thus, iron in ion-exchange process was exchanged primarily for calcium, yielded a highly dispersed catalytic iron species for coal liquefaction. Joseph et al.⁶ have shown that calcium decreases the conversion yields of coal during DCL.

Typical Mössbauer spectra of a coal containing cation-exchanged iron are shown in Figure 2. The spectra are fit with one or several magnetic components and quadrupole doublets (peak positions denoted by bar diagrams), and a superparamagnetic relaxation component (dashed curve). As discussed by Ganguly et al.⁵, at a given temperature, particles with diameter less than some critical value will give rise to a quadrupole doublet, particles with a diameter greater than some larger critical value will exhibit a six-peak magnetic hyperfine spectrum, and particles with diameters between these two values will give rise to superparamagnetic spectra. Approximate size distributions can be determined by measuring the percentages of these three components as a function of temperature. A typical size distribution determined in this manner for the cation-exchanged Beulah lignite for two different iron contents is shown in Figure 3. It is seen that the size distribution is bimodal, with a significant fraction of the iron in particles finer than 30Å in diameter and highly dispersed particles in the 30-100Å size range. In addition, the size distribution patterns of the low-iron-content cation-exchanged coals indicate the formation of the fine (less than 30Å) iron-bearing fraction in larger relative amounts. These observations imply that there are two distinct forms of iron present in these samples. The iron in the finer particle size (less than 30Å) category may in fact be ferric iron that is molecularly dispersed and bonded to oxygen anions of the carboxyl groups in the coal, while particles in the 30-100Å size range result from hydrolysis and agglomeration of either iron acetate or ion-exchanged iron to form larger iron oxyhydroxide particles.

Both the x-ray absorption near edge structure (XANES) and the radial structure function (RSF) derived from the iron K-edge XAFS spectra of the cation-exchanged coals exhibit significant size related effects. Typical results are shown in Figure 4. The XANES of cation-exchanged coals (Hagel with 5.33% and 0.88% iron content) are compared to that of bulk iron oxyhydroxide (α -FeOOH) in Figure 4a, while the corresponding RSF are compared in Figure 4b. It is seen that the XANES of the cation-exchanged iron and goethite are quite similar, with the exception of an increase in the intensity of the small pre-edge peak. This occurs because a significant fraction of the iron atoms in the coals is no longer in centrosymmetric octahedral coordination, but in reduced coordination number sites, which causes the intensity of the pre-edge ($1s \rightarrow 3d$) transition to increase⁷. This is believed to be due to surface iron atoms in the goethite particles and/or to carboxyl-bound iron atoms. The RSFs of the cation-exchanged iron in coals and iron in goethite exhibit similar peaks, but the peaks corresponding to the iron shells are decreased in amplitude for the iron in the coal. During DCL most of the cation-exchanged iron reacts with H_2S/H_2 to form pyrrhotite. In most cases, however, a small iron oxide remnant remains.

II. Development of Binary Ferrihydrite Catalysts for Direct Coal Liquefaction

Because of its unique small particle size and large surface area, the 30Å NANOCAT™ catalyst manufactured by Mach I, Inc. has attracted much interest. The 30Å catalyst is actually ferrihydrite which is one of the eight major iron

oxide/oxyhydroxide phases. The structure of ferrihydrite is still controversial. Using X-ray absorption fine structure (XAFS), we found that the structure is oxyhydroxide-like with iron octahedrally coordinated by oxygens and oxyhydroxy groups. Of more significance, a large percentage of surface iron ions are at coordinate unsaturated (CUS) sites with tetrahedral symmetry. Figure 5 shows the proposed structure.

Agglomeration and phase transition of the 30Å catalyst (ferrihydrite)

The iron oxide catalysts are in fact the catalyst precursor for coal liquefaction. Under reaction conditions, the catalyst may experience several stages of phase transformation before converting to $Fe_{1-x}S$ phase. One major concern for the iron catalysts is whether they are able to maintain their dispersion under reaction conditions. At high temperature ferrihydrite decomposes to hematite. TEM micrographs show that the 30Å catalyst after annealing at temperatures between 250 - 350°C contains two phases, a hematite phase with large particle size ($d > 200\text{Å}$) and small, apparently unaltered 30Å particles. Substantially more and larger hematite particles are observed if the samples has been exposed to moisture in the air for several day prior to annealing⁸. The phenomenon can be interpreted on the basis of surface structure. Upon exposure to moisture, water molecules are chemisorbed at the catalyst surface and the small particles become linked by the chemisorbed water. At high temperature, these water molecules are detached from the particle joints, causing agglomeration of small particles and formation of $\alpha\text{-Fe}_2\text{O}_3$ phase with decreased surface area. Detailed papers have been prepared discussing both the structure⁹ and the agglomeration and phase transition of the catalyst during annealing.

Synthesis and characterization of the binary ferrihydrite catalysts

Since the CUS sites can adsorb water molecules, they may adsorb a second element (M) if it is present during precipitation, forming M-O-Fe species at the catalyst surface. With chemisorbed water molecules, the CUS sites become the crystal growth sites; but once the CUS sites are occupied by the second element, the crystal growth sites become blocked (Figure 6), and the catalyst may be able to maintain its dispersion at high temperatures.

We have succeeded in synthesizing a series of binary ferrihydrite catalysts by coprecipitating Al, Si, Zn, and Mo with ferric nitrate. The average particle sizes of the catalysts determined by TEM micrographs are 30 - 100Å. XRD, Mossbauer spectroscopy and XAFS results show that the catalysts are structurally identical to the 30Å catalyst. TEM micrographs of the catalysts show that the nanoscale particles are heavily aggregated, whereas the 30Å catalyst particles are well separated.

To examine the effect of the second component on catalyst agglomeration, the catalysts were annealed at 400°C for 5 hours in air, and the structure of the samples before and after annealing were examined by XRD. Figures 7 and 8 show the results for pure ferrihydrite, and the ferrihydrite catalysts with 5% Mo, 5% Si, and 50% Al.

Among the compounds used as second components for coprecipitation with ferric nitrate, SiO₂ is most effective in preventing catalyst agglomeration. With Si/Fe = 5%, no α-Fe₂O₃ phase was seen after annealing at 400°C for 5 hours in air (Figure 8). With 5% of Mo, Al and Zn added to the ferric nitrate solution, crystalline α-Fe₂O₃ was observed after annealing. The particle sizes of the α-Fe₂O₃ phase estimated from the width of the XRD peaks are considerably smaller than that of pure ferrihydrite (30Å).

No formation of $\alpha\text{-Fe}_2\text{O}_3$ was seen with Al/Fe = 50%.

Coal liquefaction test results

Preliminary direct coal liquefaction tests have been performed using a tubing bomb. The conditions and product analysis are shown in Table 1. The results show that the binary catalysts are as good as or better than the 30Å catalysts. New tests with different experiment conditions and different catalyst composition are underway. A more complete summary of the results for the binary ferrihydrite catalysts have been prepared for publication^{10, 11}.

References

- 1- Taghiei, M. Mehdi; Huggins, F. E.; Ganguly, B.; Huffman G. P. *Energy & Fuels*, **1993**, 7, 399.
- 2- Taghiei, M. Mehdi; Huggins F. E.; Mahajan V.; Huffman G. P. *Energy & Fuels*, **1993**, Submitted.
- 3- Bishop, M.; Ward, D. L. *Fuel* **1958**, 37, 191.
- 4- Huggins, F. E.; Huffman, C. P. *Mössbauer Analysis of the Iron-Bearing Phases in Coal, Coke and Ash Analytical Methods for Coal and Coal Products*, Karr Jr., C. Ed, Acade. Press, NY **1979**, III, 371.
- 5- Ganguly, B.; Huggins, F. E.; Rao, K. R. P. M.; Huffman, G. P. *J. Catalysis*, in press.
- 6- Joseph, J. T.; Forrai, T. R. *Fuel* **1992**, 71, 75.
- 7- Taghiei M. Mehdi; Ph.D. Theses, Dept. of Matls. and Eng., Univ. of Kentucky, **1992**.

- 8- Feng, Z.; Zhao, J.; Huggins, F. E.; and Huffman, G. P. *J. Catal.*, in press.
- 9- Zhao, J.; Huggins, F. E.; Feng, Z.; Lu, F.; Shah, N.; and Huffman, G. P. *J. Catal.*, in press.
- 10- Zhao, J.; Feng, Z.; Huggins, F. E.; Shah, N.; and Huffman, G. P. ACS, Fuel Chem. Div. Preprint, V38, 196 (1993)
- 11- Zhao, J., Feng, Z., Huggins, F. E., and Huffman, G. P., submitted to *Energy & Fuels*.

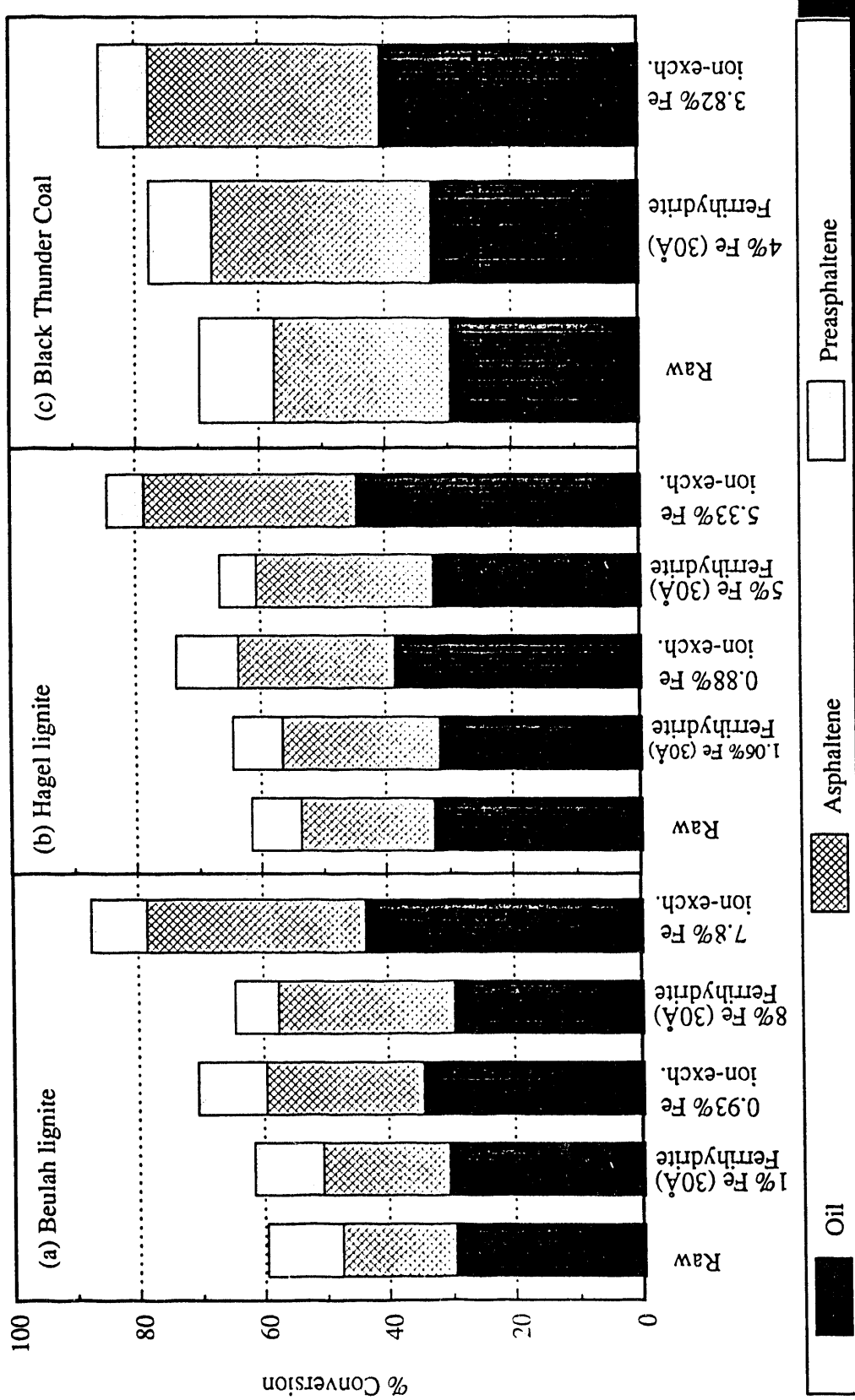


Figure 1. Comparison of liquefaction product yield for Beulah, Hagel lignites and Black Thunder coal.

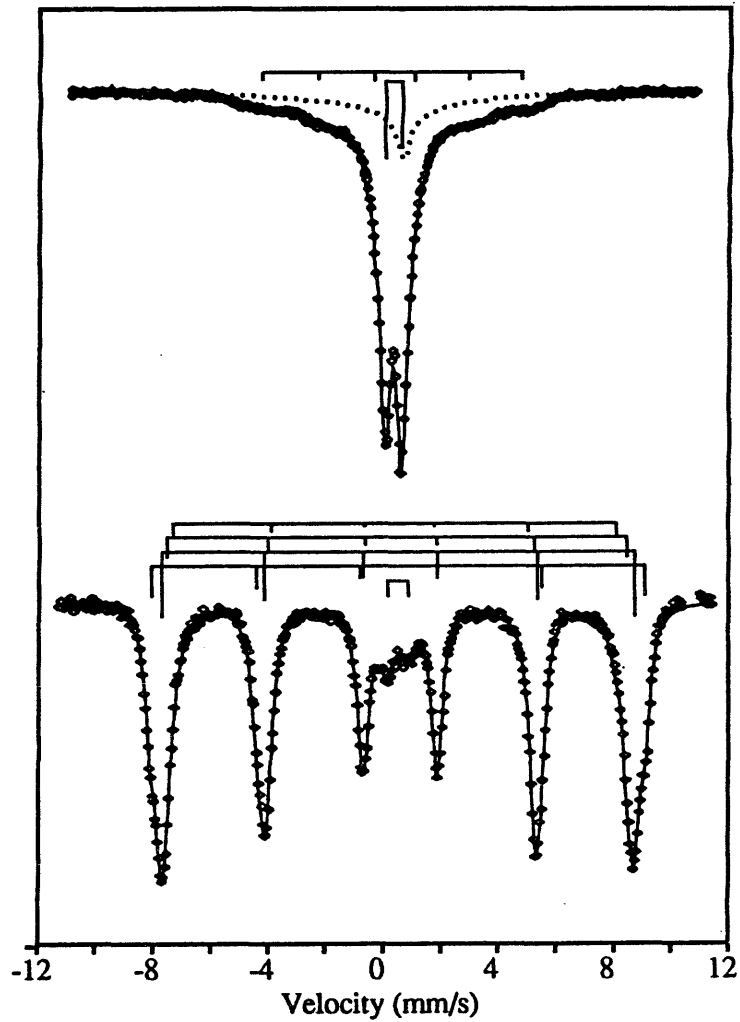


Figure 2. Mossbauer spectra of iron ion-exchanged Beulah lignite at room temperature and at 12K.

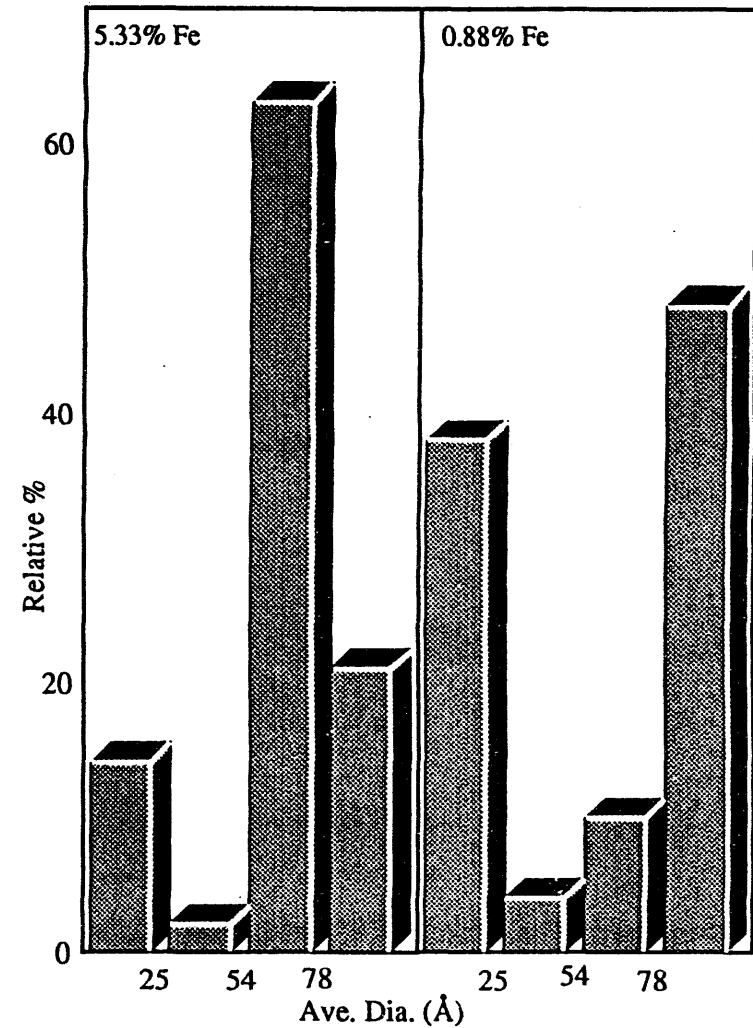


Figure 3. Size distribution of iron ion-exchanged Beulah lignite with indicated iron percentages.

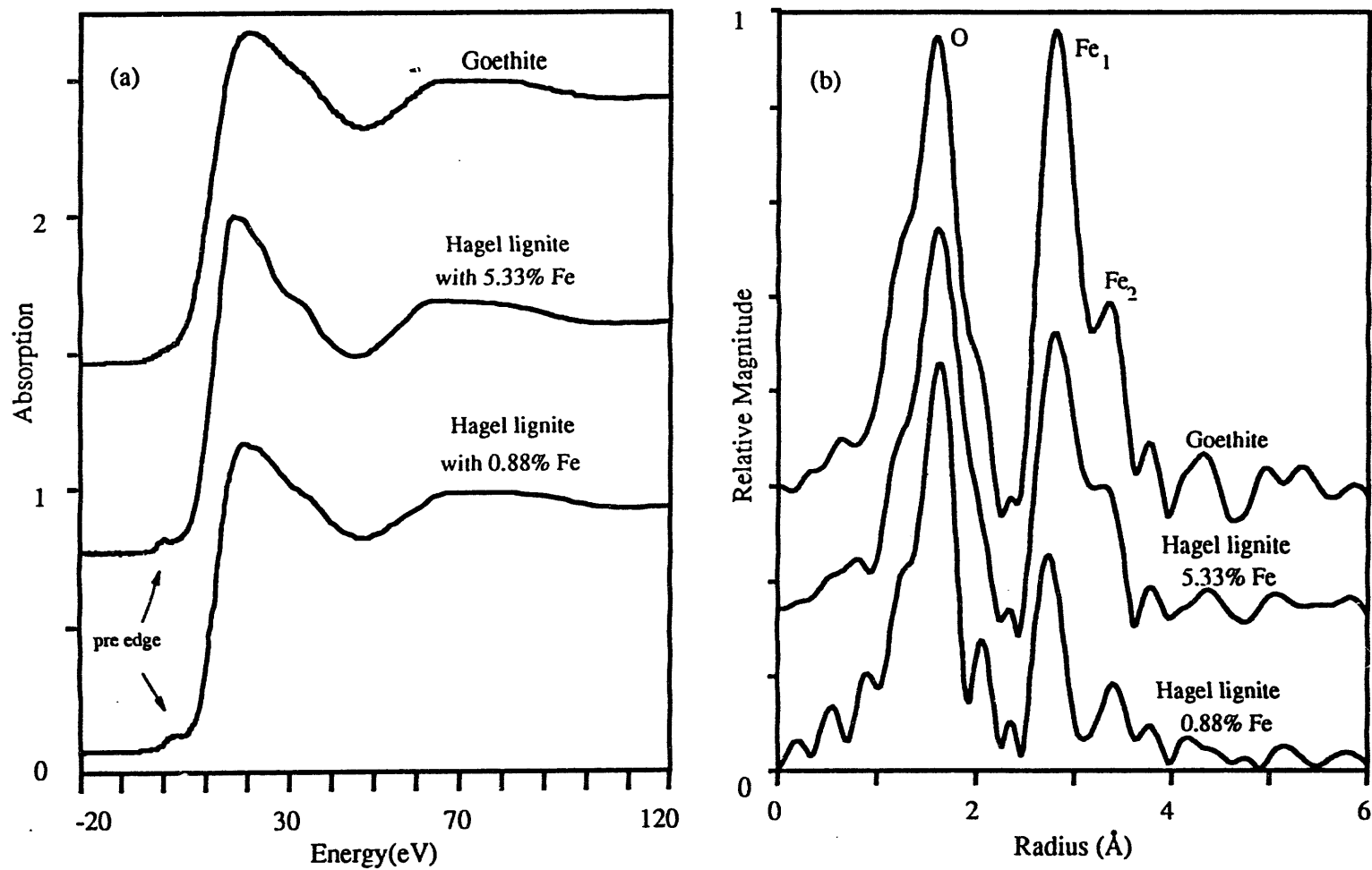


Figure 4. Comparison of (a) x-ray absorption near edge structure (XANES), and (b) radial structure function (RSF) of FeOOH and ion-exchanged Hegal lignite.

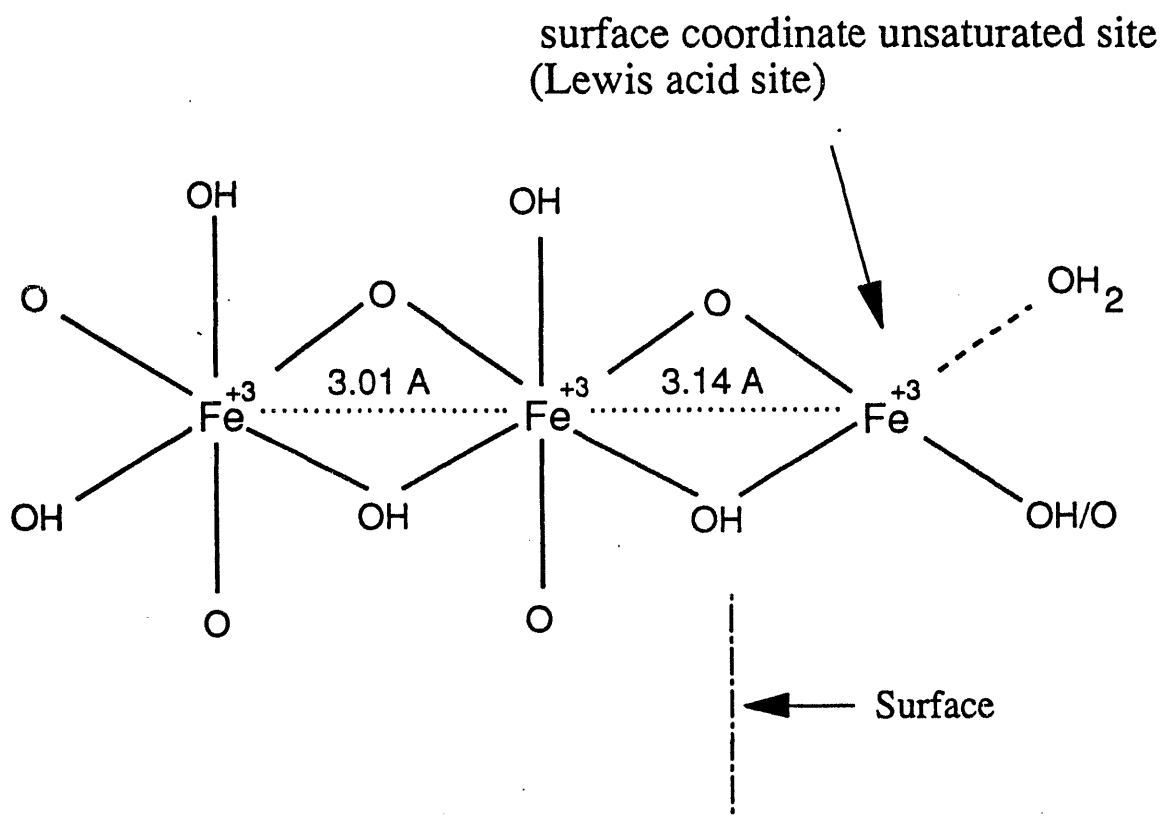


Figure 5. Proposed structural model for ferrihydrite (30 Å catalyst).

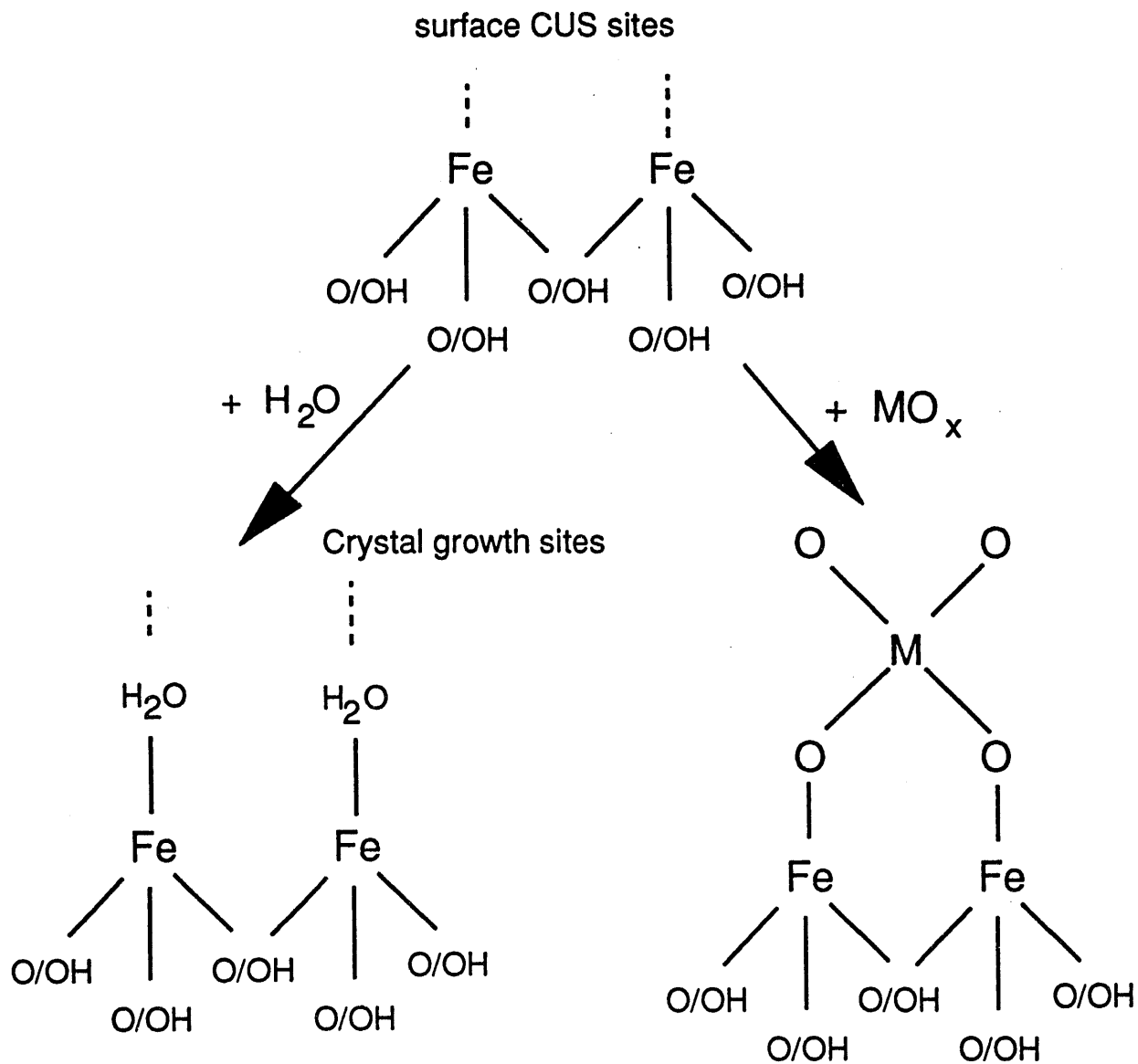


Figure 6. Chemisorption at ferrihydrite surface.

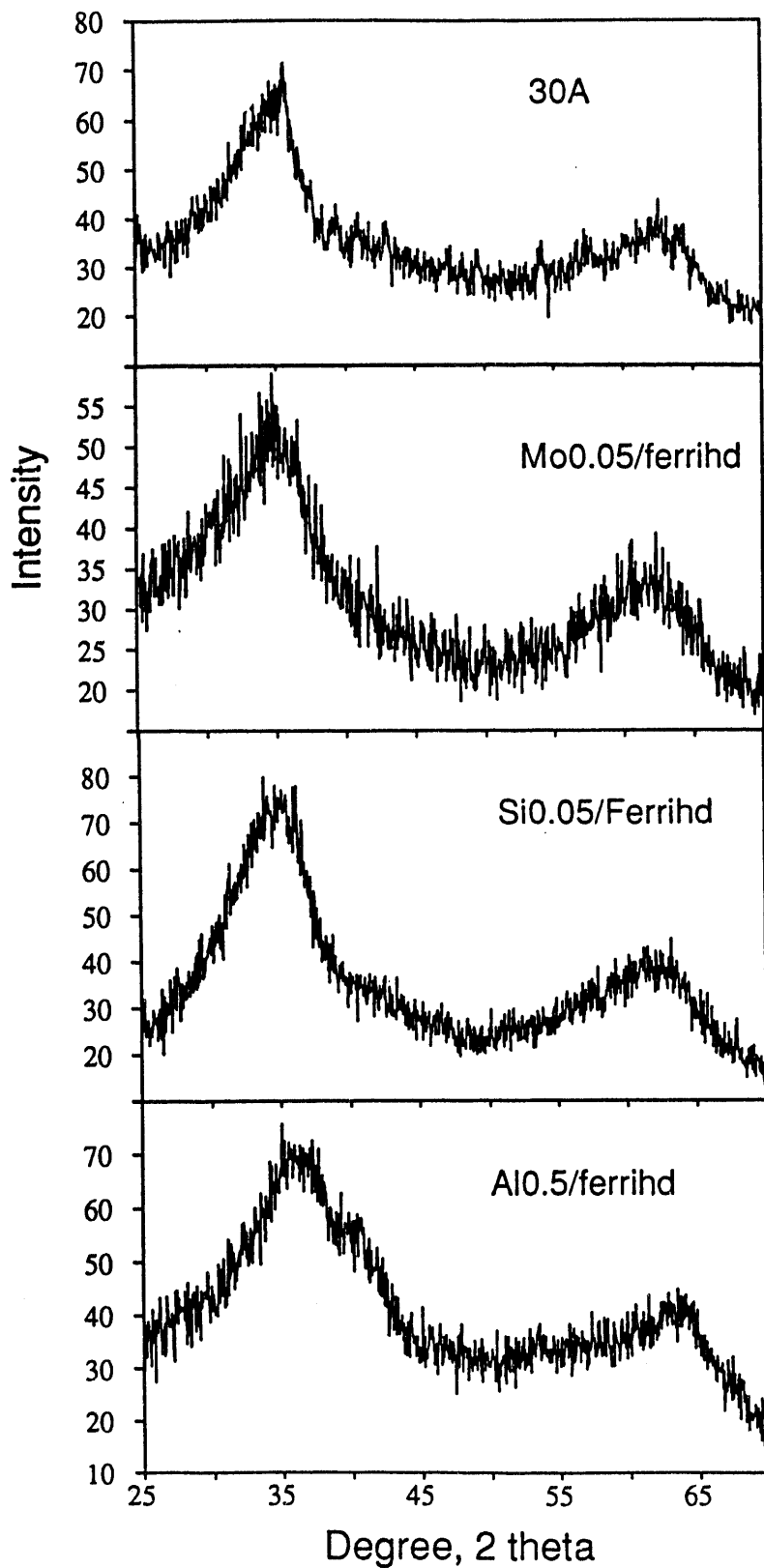


Figure 7. XRD of the 30A and the binary ferrihydrite catalysts.

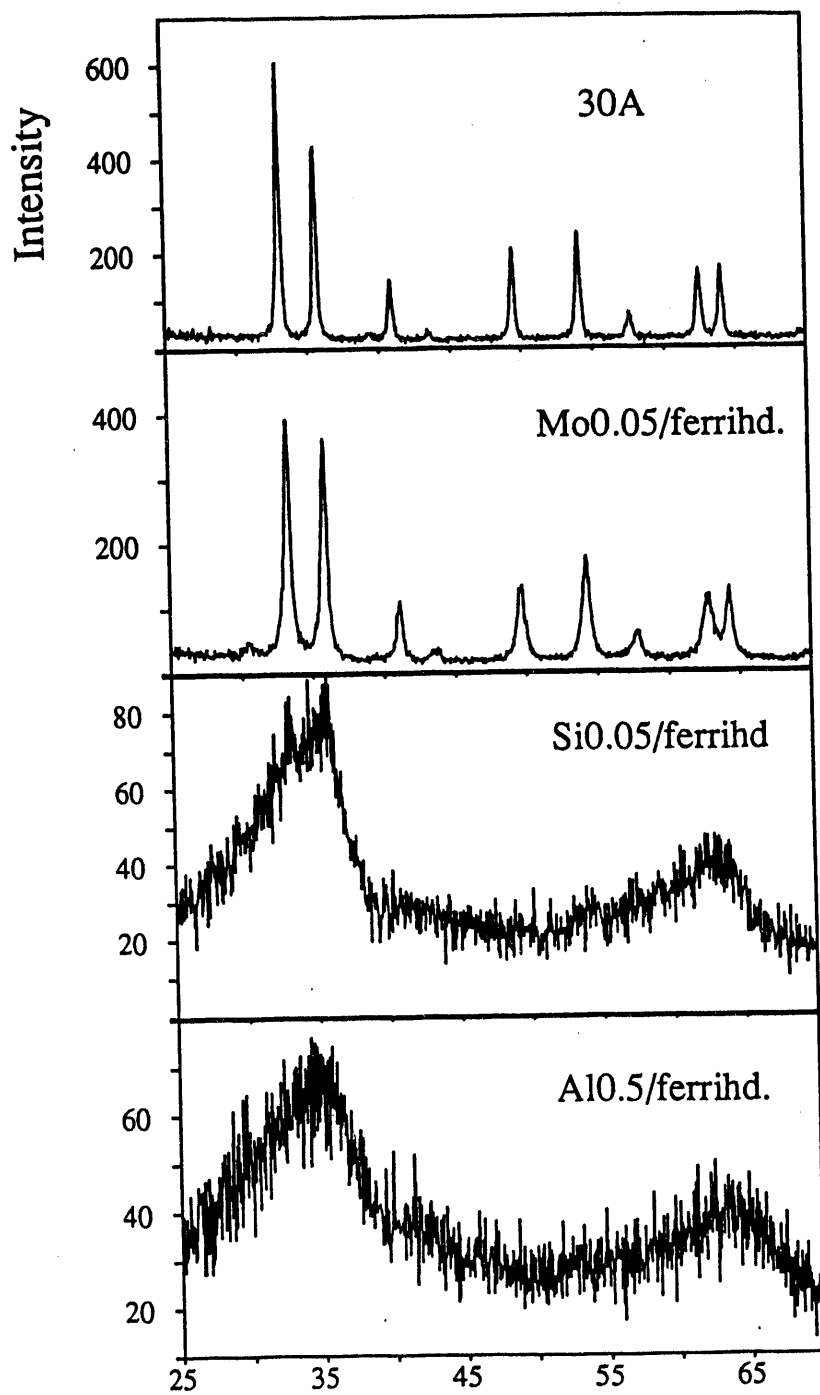


Figure 8. XRD of the binary catalysts after annealing.

Table 1. Coal liquefaction experiment conditions and products analysis.

Coal: Blind Canyon (Decs-17)
 Coal loading: 5 g
 Tetralin/Coal = 2 : 1
 Catalyst loading: Fe/Coal = 0.6%
 S(DMDS)/Fe = 2 : 1
 Reaction temp: 380°C
 H₂ Pressure: 800 psi
 Reaction time: 60 min

Liquefaction products analysis

Sample	Oil	Asphaltene	Preasphaltene	Gas	Total
30Å	18.7	42.9	9.0	2.4	73.0
ferrhydrite (M/Fe<0.01)	22.7	38.1	12.4	2.2	75.4
Si _{0.05} /ferrhydrite	23.8	40.6	7.6	2.3	74.3
Al _{0.5} /ferrhydrite	24.7	37.0	8.0	2.2	71.9

CLAY-SUPPORTED CATALYSTS FOR COAL LIQUEFACTION

Edwin S. Olson, Candace M. Buchwitz, and Mary L. Yagelowich
Universal Fuel Development Associates, Inc.
Grand Forks, ND 58201

and

Ramesh K. Sharma and Daniel C. Stanley
University of North Dakota Energy and Environmental Research Center
Grand Forks, ND 58202

Contract No. DE-AC-91PC90048

Presented at the
U.S. Department of Energy
Liquefaction Contractors' Review Conference
Pittsburgh, PA
September 27-29, 1993

ABSTRACT

In an effort to develop new disposable catalysts for direct coal liquefaction, several types of clay-supported pyrrhotite catalysts were prepared and tested. These types included iron-pillared (intercalated) montmorillonite, mixed iron/alumina-pillared montmorillonite, and iron-impregnated montmorillonite. Iron-pillared montmorillonite catalyst precursors were initially prepared by exchange of triiron clusters on fine particles of sodium montmorillonite. Agglomeration occurred with collection and sulfidation to give micron size particles, but good hydrocracking, hydrogenation, and liquefaction activity were retained. Brønsted sites on the clay were active, but the acid-catalyzed retrogressive condensation reactions normally caused by clays were prevented by the iron sulfide.

Several methods for preparing mixed iron/alumina pillared montmorillonites gave highly active catalysts. Mixed pillared clays had more stable surface areas than iron-pillared clays. Hydrogenation and hydrocracking of pyrene was comparable to that observed with zeolites and zinc chloride. Liquefaction with Wyodak coal gave improved conversions to heptane solubles (53%) compared with thermal (48%). Use of acid-exchanged Wyodak showed a small improvement in conversions. Liquefaction of Blind Canyon coal gave 37% conversion to heptane-solubles, compared with 33% for thermal reaction. Catalytic hydrogenation of a Wyodak low-severity product (3 hr) gave 47% conversion of asphaltenes to heptane solubles, compared with 26% thermal and 67% with Co-Moly catalyst.

Iron hydroxyoxide-impregnated montmorillonites were prepared from acid-washed montmorillonite. These un-pillared precursors gave highly active catalysts for hydrocracking, hydrogenation, and coal liquefaction after sulfidation. Liquefaction with Wyodak coal gave a high conversion to heptane solubles (67%), similar to Co-Moly catalyst. Acid-exchanged Wyodak gave improved conversion to heptane solubles (69%). Catalytic hydrogenation of low-severity Wyodak product (3 hr) gave 56% conversion of asphaltenes to heptane solubles, compared to 67% with Co-Moly. Thus, the most effective catalysts are those with iron sulfide on a large surface area (fine particles) of an acidic support. The combined effects of clay acidity and hydrogen activation by the pyrrhotite resulted in high conversions in hydrocracking and hydrogenation tests. The presence of pyrrhotite resulted in minimal coking and condensation reactions.

INTRODUCTION

The objective of this catalyst research program is the development of disposable, highly dispersed, high surface area catalysts for the direct liquefaction of coal. These catalysts consist of small pyrrhotite clusters intercalated into or supported on smectite clays. The clay supporting materials are highly useful in many chemical applications because of their small particle size ($< 2 \mu$), appreciable surface area for adsorption of organic molecules, and unique intercalating capabilities and are therefore utilized for supporting microcrystalline or metal cluster catalytic sites. Acidic smectites were used as petroleum-cracking catalysts for many years (1).

The smectite clays can be intercalated by large hydroxylated or complexed metal cations that pillar the aluminosilicate layers of the clays, resulting in the formation of large microporous networks analogous to zeolites. These structures may be stable up to 500°C in contrast to the non-pillared clays, which dehydrate and collapse at temperatures over 200°C. The advantage of the pillared clay catalysts over the more thermally stable zeolites is that pore size can be controlled and made larger than that of most of the zeolites. It is hoped that these pillared clay catalysts may be more effective in cracking the large coal macromolecules than the conventional catalysts. The intent of this work is to discover how to obtain finely dispersed iron sulfide (pyrrhotite) catalytic sites in the pillared clay structure that will be useful for coal liquefaction.

RESULTS AND DISCUSSION

Iron-Pillared Clays

Preparation methods for iron-pillared montmorillonites were initially investigated. Sodium montmorillonite disperses to an extremely fine particle size in an aqueous medium with low concentrations of base. The clay layers are separated (dispersed and deflocculated) in this state and mass transfer is rapid, thus this form was preferred for metal ion exchange reactions for producing the intercalated clays. The monocationic polyoxytriiron (III) complex (heptaacetatohydroxytriiron nitrate) was exchanged for the interlayer cations of the dispersed sodium montmorillonite (2). The exchange of polyoxytriiron for sodium resulted in a change in particle-size distribution, with a substantial portion of larger particles being formed by

flocculation of the very fine particles. Light scattering determination of the particle size gave an average particle size greater than 1 micron. Low-speed centrifugation gave a larger particle fraction (78%), and a fine particle fraction was isolated by high-speed centrifugation.

Calcination of the two iron-exchanged clay fractions gave the stable polyoxyiron cation-pillared clays, which were the precursors for the iron sulfide catalysts. X-ray diffraction studies of both calcined catalyst precursor fractions showed that hematite and maghemite (both Fe_2O_3) had formed. The material from the fine clay particles contained hematite in greater abundance than that from the larger particles. The formation of these different compositions during the calcination of the iron-exchanged clays may be attributed to partial hydrolysis of the triiron clusters during washing and collection procedures. The fine particles were exposed to water for a much greater period of time. These data appear to be similar to those obtained by Lee and others (3) for pillaring with hydrolyzed ferric chloride, which indicated that hematite particles had formed. The d_{001} peak corresponding to the interlayer spacing was present, but was quite broad in the 2θ plot for both samples, indicating that spacings are irregular in the calcined products. Thus, the exchange of the triiron complex results in both oriented aggregation to form pillared structures, but also flocculation to large particles with irregular edge-to-face and edge-to-edge associations of the pillared structures.

When a more rapid method for centrifugation of the fine particles was employed, the X-ray diffraction data showed that the calcined clays from the fine particles had a much smaller amount of hematite than the clay prepared by the former method. Thus, the iron oxide compositions of catalyst precursors obtained from both the fine and larger particles in this preparation were very similar.

Conversions of the oxyiron-intercalated clays to active sulfide forms were performed by various methods. Sulfidation was carried out either by heating the calcined precursor with a mixture of H_2S (100 psi) and H_2 (900 psi) in the rocking heater at 400°C for 2 hr or by in situ reaction with 40 mg of carbon disulfide that was added with the test compound, decalin solvent, or coal, depending on the reaction being carried out. The catalysts prepared by treatment with H_2S exhibited major peaks corresponding to pyrrhotite. The pyrrhotite peaks were relatively narrow, indicating that the particle size of the iron sulfide in the catalyst may be larger than desired for high catalyst activity. Sulfidation under these conditions may have mobilized the iron in the pillars so that some larger iron sulfide particle formed, as described by Lee and others (3). In contrast, the catalysts activated by in situ treatment with CS_2 did not show significant peaks for pyrrhotite or pyrite. Since sulfidation did occur, the iron sulfide species in these catalysts must be very minute. As described below, these catalysts had superior hydrocracking activities.

Surface areas of the fine particle and large particle iron-pillared clay catalysts were 156 and $181 \text{ m}^2/\text{g}$, respectively. However, on sulfiding the fine particle iron-pillared clay catalyst in H_2S and H_2 at 400°C for 2 hours, the surface area dropped to $17 \text{ m}^2/\text{g}$. The reduction in surface indicates an undesired collapse of the interlayer structure as the sulfide forms.

The hydrocracking activities of iron-pillared clay catalysts were determined by reactions with bibenzyl as the test compound. The reactions were carried out at 350°C for 3 hours in the presence of 1000 psi of molecular hydrogen in a 10-ml rocking autoclave reactor. Initially tests were conducted with 50 wt % catalyst in the bibenzyl, but later the tests used 10% catalyst concentrations. The catalysts were recovered in quantitative amounts, and no retrograde cationic condensation products or coke were observed during reactions.

A comparison of the bibenzyl hydrocracking results for the initial sulfided catalysts prepared from the fine and larger iron-pillared clay particles showed that the catalyst from the hematite-containing fines had a much lower activity (62% conversion) than the catalyst from the large particles (80% conversion). The lower activity of the catalyst from the fines was attributed to hydrolysis reactions that occurred prior to calcining. For the second batch of pillared clays that were rapidly collected, the bibenzyl hydrocracking activities of the sulfided catalysts were essentially identical for the fine and larger particles (79 and 80% conversion, respectively). This observation was consistent with the low hematite content of both precursors as demonstrated by the similar 2θ plots described above.

Examination of the products obtained from the reactions of bibenzyl with sulfided iron-pillared clays provided information on the nature of the hydrocracking activity for the catalysts. The major products were benzene, toluene, and ethylbenzene. Benzene and ethylbenzene were the largest products, and the amount of benzene was considerably more than ethylbenzene, indicating the further cracking of the ethylbenzene to benzene. These products are indicative of the Brönsted acid catalysis mechanism. The mechanism involves the ipso protonation of an aromatic ring of bibenzyl, followed by aryl-methylene bond cleavage to form benzene and phenylethyl carbonium ion. The phenylethyl carbonium ion is reduced to ethylbenzene by hydride transfer or hydrogenation, or it could undergo a variety of reactions to give other products. This reaction mechanism is common in reactions catalyzed by clays and clay-supported catalysts. The formation of toluene probably occurs via a Lewis acid catalyzed mechanism, since the temperature is too low for homolytic cleavage of the central bond in bibenzyl. Reduction of carbonium ion intermediates in the reaction may or may not involve the iron sites.

The bibenzyl cracking products included many hundreds of other components, indicative of rearrangements and hydrogen addition as well as hydrocracking. Part of the single-ring aromatics was hydrogenated to give cycloalkanes in the reactions with sulfided catalysts. A substantial amount of methylcyclohexane was formed, probably from cleavage of the tertiary carbonium ion derived from phenylethylcyclohexane or hydrogenation of the ring-protonated bibenzyl. Minor components formed as a result of hydrocracking were propylbenzene, butylbenzene, tetralin, ethylbibenzyl, and phenylethylbibenzyl, etc. The alkylbenzene products resulted from hydrogenation of bibenzyl followed by cracking reactions, probably involving Lewis acid sites.

A second factor in determining the activity of the catalysts was the concentration of iron introduced into the clay. Use of a smaller amount of iron might result in a lower number of pillars and, consequently, result in a larger micropore volume. Exchange of one-third of the total equivalents of sodium by the triiron acetate cation rather than using an

excess of the triiron gave a catalyst, after calcination and sulfidation of the large particle fraction, that was as active in hydrocracking reactions (79% conversion) as the catalyst prepared previously with excess triiron complex. The fine particle fraction had a lower activity (33% conversion).

The presence of excess sodium cations in the catalyst resulted in a serious loss of activity due association of the sodium with Brönsted acid sites in the clay or pillar. The sodium ions were exchanged out of one of the clays (from the fine particles) with ammonium ions following the iron-exchange. Calcination of this precursor to drive off ammonia gave a more active catalyst (64% conversion compared with 33%), because of regeneration of the Brönsted acid sites.

A comparison of the sulfided versus nonsulfided forms of the iron-pillared clays showed that the nonsulfided forms had a much lower hydrocracking activity (36 and 40% conversions for fine and large particles, respectively). These values are consistent with those obtained for other clay supports. Major products from nonsulfided catalysts were the same as those obtained with sulfided catalysts. The major difference in activity for the nonsulfided clays was the lower conversion, lower amounts of cyclohexanes, and lower proportion of ethylbenzene. Some of the reaction products were addition products of bibenzyl that may be regarded as Friedel Crafts addition products. However, extensive condensation and coke formation were not observed in the reaction. In comparison, acidic clay catalysts gave larger amounts of condensation products. Our results indicate that iron-pillared clays are effective in cleaving aryl-methylene and other C-C bonds at lower (350°C) temperature.

Mixed Iron/Alumina-Pillared Montmorillonites

A general problem with the iron-pillared clays is that the calcination and/or sulfidation treatments appear to mobilize the iron and generate particles of the iron oxide and sulfide that are larger than desired for maximum utilization of the iron. Surface areas are substantially decreased, owing to collapse of the layer structure. The use of discrete mixed alumina/iron-pillared clays or of alumina-pillared clays as supports for pyrrhotite active sites may give a more effective particle size for the iron sites and more stable pillared structures. The aluminum pillars are stable to calcining and sulfidation treatments.

Aluminum pillars were introduced by treatment of sodium montmorillonite dispersions with the oxyaluminum cation, and various methods were investigated for intercalation of the iron. Several pillared clay catalysts with discrete pillars composed of alumina and of iron oxide were prepared by intercalation of sodium montmorillonite first with oxyaluminum cations and then with oxyiron cations (sequential pillaring). These materials differed in the amounts of alumina and iron oxide introduced. After calcining and sulfiding with hydrogen sulfide/hydrogen mixture, these catalysts exhibited high activities, with conversions of 85 to 88% in hydrocracking tests with bibenzyl. Neither the concentration of alumina or iron had a significant effect on the activities, and a relatively low iron concentration (500 ppm) was quite active in the tests.

A second method for preparation of the discrete pillars was utilized. In this method, the oxyaluminum cations and the oxyiron cations were added simultaneously to the sodium montmorillonite in large excess. The catalyst obtained by calcining and sulfiding as above was nearly equally effective in hydrocracking tests with bibenzyl (83% conversion). Thus either the simultaneously or sequentially mixed pillared clays gave stable clays containing effective concentrations of pyrrhotite and acidic sites for catalysis.

The third method for preparing mixed pillared clays utilized a mixed oxymetal cation complex composed mainly of aluminum with a small amount of iron. This alloy-pillaring gave a catalyst with lower activity in hydrocracking tests (72% conversion). X-ray diffraction showed that iron from the alloy pillar had been converted to pyrrhotite by the sulfidation; hence, the lower activity is probably due to some collapse of the pillared structure during this transformation of the iron.

Since the presence of sodium ions was found to exert a significant negative effect on hydrocracking conversion, one of the sequentially pillared catalysts was treated with ammonium nitrate in order to exchange out any remaining sodium ions. After calcination to volatilize the ammonia and sulfidation, the catalyst gave a slightly better conversion in the bibenzyl hydrocracking test (89%).

The method of sulfiding the iron in the mixed metal-pillared catalyst was also varied. By adding a small amount of carbon disulfide to the reaction rather than presulfiding the catalyst with hydrogen sulfide/hydrogen, a significantly higher conversion of bibenzyl was obtained (94%). The reason for higher activity is suspected to be that the pyrrhotite particle size is smaller with this method of sulfiding (see discussion above).

In addition to effective catalysis of hydrocracking reactions at moderate temperatures, the iron-pillared clays were effective catalysts for catalyzing the hydrogenation of pyrene. Hydrogenation of pyrene with a sulfided (H_2S/H_2) iron-pillared clay catalyst at 350°C for 3 hr gave an 88% conversion to hydrogenated pyrenes. The hydropyrene yields were better than those obtained with sulfided nickel molybdenum under identical conditions (69%). Conversion to the hexahydropyrenes had not proceeded very far in the latter case. A mixed metal-pillared catalyst was tested with pyrene at 400°C in the rocking microreactor with 1000 psi of hydrogen (measured at room temperature). A 68% conversion of the pyrene was obtained. The lower yield is consistent with the smaller equilibrium constant for hydrogenation at the higher temperature. Importantly, hydrocracking of the hydrogenated pyrenes was observed (36%) at 400°C. At 440°C, the conversion of pyrene dropped to 50%, and the yield of hydrocracked products increased (47%).

Liquefaction testing with Wyodak subbituminous coal in tetralin solvent was performed with the discreet iron/alumina-pillared catalyst. The liquefaction reaction was carried out at 425°C for 1 hr in a 71-mL reactor with 1000 psi hydrogen (measured at ambient temperature). The catalyst was sulfided by adding a small amount of carbon disulfide. THF insolubles and pentane insolubles were measured by weighing. The pentane solubles contained the tetralin solvent; therefore, the oil yield was determined by the difference between the isolatable products described above and the maf coal weight (thus the amount

includes gases and reaction product water). For this reaction, yields of THF solubles were 19%, toluene solubles were 25%, and oils/gases were 46%, with a total conversion to soluble products of 90%. These yield data are approximately the same as the thermal (no catalyst) data.

In an effort to improve the performance of the clay-supported iron catalyst, the preparation method was modified in several ways. One modification involved addition of the triiron complex to an alumina-pillared clay, rather than hydrolyzed ferric nitrate. The resulting discreetly pillared clay (Fe_3APC) exhibited very high activities in hydrocracking tests with bibenzyl at 10% catalyst concentrations. Depending on the preparation methods, the bibenzyl conversions ranged from 84 to 98% and yields of benzene were high. Despite the high activity, not much condensation to higher molecular weight products occurred. Addition of triiron to the zirconia pillared clay gave a catalyst with lower activity in the bibenzyl cracking test. The Fe_3APC catalyst was also effective for pyrene hydrogenation and cracking.

Liquefaction tests with the Fe_3APC catalyst (in situ sulfiding) were carried out with both as received (ARW) and acid-exchanged Wyodak (IEW) coal. The conversion to THF solubles for the ARW was 91% with 53% heptane solubles. The conversion with the IEW was better (95%), but yields of heptane solubles were about the same (54%). Thus, the calcium in the low-rank coal did not contribute to extensive poisoning of the catalyst in this test. These data for the Fe_3APC catalyst may be compared with liquefaction data obtained in the same reactors and conditions but with a dispersed iron catalyst prepared by the PETC method. The reaction of ARW using the PETC iron impregnation method gave 88% conversion to THF with 52% heptane solubles, whereas the IEW with the PETC method gave 91% conversion to THF soluble with 56% heptane solubles. Thus, the calcium poisoning appears to be significant for the dispersed iron catalyst.

For a reaction where the Fe_3APC catalyst was not sulfided, the conversion and heptane-soluble fraction dropped to 87% and 33% respectively. The reason why the conversion and yield drop below the thermal reaction values is that the highly acidic clay catalyzed retrogressive reactions. In contrast, when the highly dispersed iron sulfide is present on the clay, hydrogen is transferred to the cations generated on the clay acid sites, and reduction rather than condensation occurs.

The liquefaction of Blind Canyon coal was also investigated with the Fe_3APC catalyst. The conversion to THF solubles was 92% with 37% yield of heptane solubles. These data show a catalytic effect over the thermal reaction data, 91% conversion with 33% yield of heptane solubles.

To further evaluate the effectiveness of the mixed iron/alumina pillared clays for catalyzing hydrogenation and depolymerization reactions, conversion data for a solubilized coal intermediate was obtained and compared with that from other dispersed iron and molybdenum catalysts.

Several reactions of a mineral-free low-severity intermediate from Wyodak coal (LSW) were carried out with the iron catalysts. A THF-soluble intermediate was obtained by thermal liquefaction in tetralin solvent with CO/H₂S and was separated from heptane-soluble products and solvent-derived materials by solvent (heptane) precipitation to give the high molecular weight LSW intermediate for these tests. The LSW is a low-density solid at ambient temperature, but melts easily. Since the substrate contains no heptane-soluble oils, the conversion of the asphaltenes to heptane-soluble oils can be readily determined in the product.

A thermal (noncatalytic) reaction of the LSW in tetralin at 425 °C for 1 hr in 1000 psi hydrogen gave 15% conversion to heptane-solubles (Table 1). The 15% value for the LSW substrate represents a conversion of preasphaltenes and asphaltenes to mainly heptane-soluble oils and a small amount of water, but essentially no formation of carbon dioxide and hydrocarbon gases. A small amount of hydrogen transfer from the tetralin solvent is believed to occur and is accompanied by some dehydration to give a somewhat more soluble product.

The liquefaction reaction of the LSW in tetralin with the mixed iron/alumina-pillared clay catalyst (in situ sulfided) gave 30% conversion to heptane-solubles under the same conditions. The weight of catalyst used corresponded to 10% of the weight of low-severity intermediate; the iron content used in the reaction was thus 1% of the intermediate. This ratio is the same as that used in reactions with the coals. Since the catalyst can be easily recovered from the second stage reaction, it might be used in much greater amounts in an actual process; however, the ratio was kept low in these experiments to provide more discriminating data for catalyst evaluation.

The two-fold increase in conversion to oils for catalytic versus thermal reactions with the LSW substrate can be attributed to both hydrocracking and hydrogen transfer reactions catalyzed by the sulfided iron (pyrrhotite) on the highly acidic pillared clay support. Depolymerization of the coal is impossible to measure directly for small amounts of substrate in a donor solvent, because of inaccuracies in both distillation and GC methods.

Iron-Impregnated Montmorillonite

Because the combinations of pyrrhotite with clay exhibited good hydrocracking and hydrogenation catalysis with model compounds, but were only moderately successful with Wyodak coal, an alternative method for supporting iron on the clay was investigated. Addition of either triiron complex or ferric nitrate to an acid-washed montmorillonite followed by hydrolysis by ammonia addition gave the iron hydroxyoxide-impregnated clay precursor. More of the iron should be on the surface faces and edges of the clay and less in the interfacial volumes than was the case for the pillared clays.

The activities of the iron-impregnated montmorillonites were tested with bibenzyl (in situ sulfidation). The Fe₃-impregnated K-10 montmorillonite (Fe₃K10) gave a higher conversion (65%) than the ferric-impregnated K-10 montmorillonite (IMont). These conversions were lower than those obtained with the mixed iron/alumina pillared clays. This

difference could be attributed to the higher acidity of the pillared clay support. Hydrogenation activity was tested with pyrene at 400°C (in situ sulfidation). The IMont catalyst gave a good conversion to hydroxyrenes and a somewhat lower amount of cracked products, compared with the mixed iron/alumina pillared montmorillonites. Again this difference in activity can be attributed to the higher acidity of the pillared clay supports.

Liquefaction of Wyodak coal with the iron-impregnated clays gave high conversions to THF solubles as well as heptane solubles. Initial tests with IMont catalyst with as received Wyodak gave 93% conversion to THF solubles and 67% conversion to pentane solubles. The test was repeated with another batch of IMont which resulted in the same conversion 93% to THF solubles and 67% to heptane solubles. Liquefaction of an acid-exchanged Wyodak sample gave 95% conversion to THF solubles and 69% to heptane solubles. The Fe₃K10 gave 92% conversion to THF solubles and 57% to heptane solubles.

Liquefaction testing was also performed with these catalysts to determine the depolymerization activity with the Wyodak low-severity intermediate. The IMont catalyst gave 45% conversion of the LSW asphaltenes to heptane-soluble oils. As in the tests with as received and acid-exchanged Wyodak liquefaction discussed above, the activity of the IMont in the LSW liquefaction is substantially higher than that of the mixed iron/alumina pillared catalyst. The activity of the IMont is a little lower than that of commercial cobalt/molybdenum catalyst (51% conversion to heptane solubles).

The IMont catalyst contains 10% iron by weight. Since the hydrocracking activity for the reaction with bibenzyl is similar to that of the mixed iron/alumina-pillared montmorillonite catalyst, the higher activity of the IMont with LSW and also with the initial Wyodak coal (both as-received and acid exchanged) can be attributed to a higher effective iron concentration on the surfaces available to the coal-derived macromolecules. Much of the iron intercalated into the pillared clay may not actually be accessible after sulfidation or at the reaction is diffusion limited.

A commercial supported cobalt-molybdenum was also tested for reactivity with the low-severity intermediate. The conversion to heptane solubles with a comparable amount of the sulfided cobalt-molybdenum catalyst was 51%. This catalyst is known to have high activities for hydrogen activation and hydrogen transfer from donor solvent to the coal (). In an earlier report (Toronto), the conversion of a similar low-severity Wyodak intermediate was substantially higher (66% to pentane solubles), but much more catalyst was used in these studies (weight cat./weight LSW = 1).

SUMMARY AND CONCLUSIONS

A. Iron-pillared clay catalysts.

- 1. Catalysts prepared by exchange of triiron clusters on montmorillonite and in situ sulfidation gave catalysts with high hydrocracking activity.**

2. **Hydrocracking activity in iron-pillared clays was highest when prepared by rapid collection and rapid drying of particles and ammonia treatment.**
3. **Hydrocracking activity is related to Bronsted sites on the clay as well as maghemite content of intermediate oxide.**
4. **Iron-pillared clays are effective catalysts for hydrogenation and prevent the acid-catalyzed retrogressive condensation reactions that occur with clays.**

B. Mixed iron/alumina-pillared clay catalysts.

1. **Several methods for preparing mixed iron/alumina pillared montmorillonites gave highly active catalysts.**
2. **Mixed pillared clays had more stable surface areas following sulfidation than iron-pillared clays.**
3. **Hydrogenation and hydrocracking of pyrene was comparable to that observed with zeolites and zinc chloride.**
4. **Liquefaction with Wyodak coal gave improved conversions to heptane solubles (53%) compared with thermal (48%).**
5. **Use of acid-exchanged Wyodak showed a small improvement in conversions.**
6. **Liquefaction of Blind Canyon coal gave 37% conversion to heptane-solubles, compared with 33% for thermal reaction.**
7. **Catalytic hydrogenation of a Wyodak low-severity product (3 hr) gave 47% conversion of asphaltenes to heptane solubles, compared with 26% thermal and 67% with Co-Moly catalyst.**

C. Iron-impregnated clay catalysts.

1. **Iron hydroxyoxide-impregnated montmorillonites were prepared which gave highly active catalysts for hydrocracking, hydrogenation, and coal liquefaction after sulfidation.**
2. **Liquefaction with Wyodak coal gave high conversion to heptane solubles (67%) similar to Co-Moly catalyst.**
3. **Acid-exchanged Wyodak gave improved conversion to heptane solubles (69%).**
4. **Catalytic hydrogenation of low-severity Wyodak product (1 hr) gave 45% conversion of asphaltenes to heptane solubles, compared to 51% with Co-Moly.**

REFERENCES

1. Ryland, L.B.; Tamale, M.W.; Wilson, J.N. Catalysis; Emmett, P.H. Ed.; Reinhold: New York, 1960, Vol. 7, Chap. 1.
2. Yamanaka, S.; Doi, T.; Sako, S.; Hattori, M. Mat. Res. Bull. **1984**, 19, 61-168.
3. Lee, W.Y.; Raythatha, R.H; Tatarchuk, B.J. J. Catal. **1989**, 115, 159-179.